ESA/Contract No. 4000126561/19/I-NB

Consortium Members

ESA Sea Level CCI+

Product Validation and Inter Comparison Report

Reference:	
Nomenclature:	SLCCI+_PVIR_018_ProductValidation
Issue:	2.1
Date:	Sep. 3, 21

European Space Agency

Chronology Issues:			
Issue:	Date:	Reason for change:	Author
1.0	02/03/20	Initial Version	NOC, LEGOS, CLS
2.0	30/07/21	Annual update	NOC, LEGOS, CLS
2.1	03/09/21	Improvements after review comments	NOC, LEGOS, CLS

People involved in this issue:			
Written by:	A. Cazenave;F. Calafat; P Prandi		
Checked by:	JF Legeais (CLS)		
Approved by:	JF Legeais (CLS)	17/09/2021	

Acceptance of this deliverable document:			
Accepted by ESA:	J. Benveniste (ESA)	Date: 2021.10.07 '16:50:03 +02'00	Digitally signed by Jérôme Benveniste

Distribution:		
Company	**Names**	**Contact Details**
ESA	J. Benveniste A. Ambrozio, M. Restano	Jerome.Benveniste@esa.int; Americo.Ambrozio@esa.int; Marco.Restano@esa.int
CLS	J.-F. Legeais ; P. Prandi ; S. Labroue ; A. Guerou	jlegeais@groupcls.com ; pprandi@groupcls.com; slabroue@groupcls.com; aguerou@groupcls.com;
LEGOS	A. Cazenave ; B. Meyssignac ; F. Birol; F. Nino; F. Leger;	anny.cazenave@legos.obs-mip.fr; yvan.gouzenes@legos.obs-mip.fr; Benoit.Meyssignac@legos.obs-mip.fr; florence.birol@legos.obs-mip.fr; fernando.nino@legos.obs-mip.fr; fabien.leger@legos.obs-mip.fr;
NOC	F. Calafat	Francisco.calafat@noc.ac.uk;
SkyMAT Ltd	Andrew Shaw	agps@skymat.co.uk;
DGFI-TUM	Marcello Passaro	marcello.passaro@tum.de; Julius.oelsmann@tum.de

List of Contents

1. Introduction

The objective of this report is to summarize the inter comparison and validation results of the sea level datasets generated during the extension of the ESA Sea Level Climate Change Initiative program (SL_cci+). The goal here is to certify the quality of the final datasets distributed to the users.

Initially, a 16-year-long (June 2002 to May 2018), high-resolution (20-Hz), along-track sea level dataset at monthly interval, together with associated sea level trends, had been computed at 429 coastal sites in six regions (Northeast Atlantic, Mediterranean Sea, West Africa, North Indian Ocean, Southeast Asia and Australia). This preliminary coastal sea level product (called **version 1.1**) was based on complete reprocessing of raw radar altimetry waveforms from the Jason-1, Jason-2 and Jason-3 missions. It was published in November 2020 in the Nature Scientific Data journal (the Climate Change Initiative Coastal Sea Level Team, Coastal sea level anomalies and associated trends from Jason satellite altimetry over 2002-2018, *Nature Scientific Data*, 7, 357, https://doi.org/10.1038/s41597-020-00694-w, 2020.) and the products are available from the SEANOE website (https://doi.org/10.17882/74354). A focus on a specific case (the Senetosa site) has also be the object of a publication (Gouzenes et al., 2020).

The processing methodology, the statistics on the computed coastal trends over 2002-2018 (version 1.1) and the validation with tide gauges are presented in annex 1 (section 5).

A new product (called **version 2.0**) has been recently computed and planned to be distributed after full validation during autumn 2021. This is an extension both in time and space of the version 1.1. It covers a full 18 year-long time span: January 2002 to December 2019, and in addition to the previous 6 study regions, now covers the whole African continent. The processing methodology is the same for both versions.

In addition, the SL_cci+ activity has also focused on the characterization of the uncertainties of the regional sea level trends. This work is briefly presented in Annex 2 (section 6) and the full results are presented in Prandi et al., Local sea level trends, accelerations and uncertainties over 1993–2019. Sci Data 8, 1 (2021). https://doi.org/10.1038/s41597-020-00786-7

2. Extended coastal sea level trends over 2002-2019 (version 2.0): new results

Here we briefly present the current status of the version 2.0 product.

Figure 1 shows the new study regions.

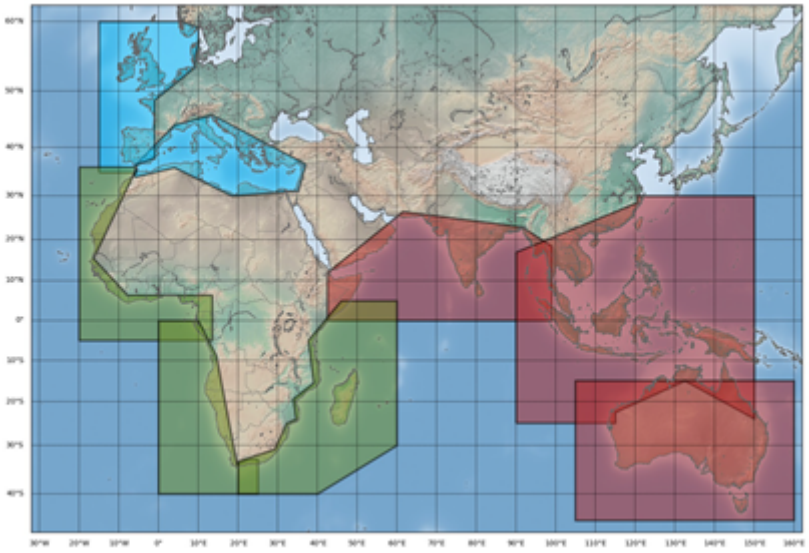

Figure 1*: Map of the study regions*

Using the extended along-track time series, coastal sea level trends have been computed over January 2002 to December 2019. A total of 620 sites have been selected.
Figures 2 and 3 show shortest distance to the coast reached in the version 2.0 product, and the associated coastal trends.

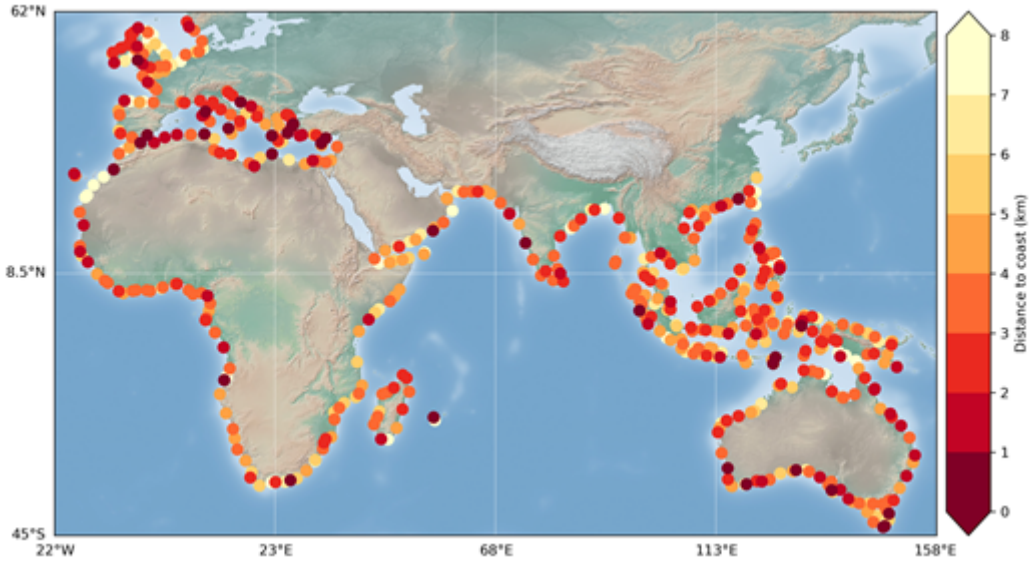

Figure 2*: Shortest distance (km) to the coast of the first valid trend estimate*

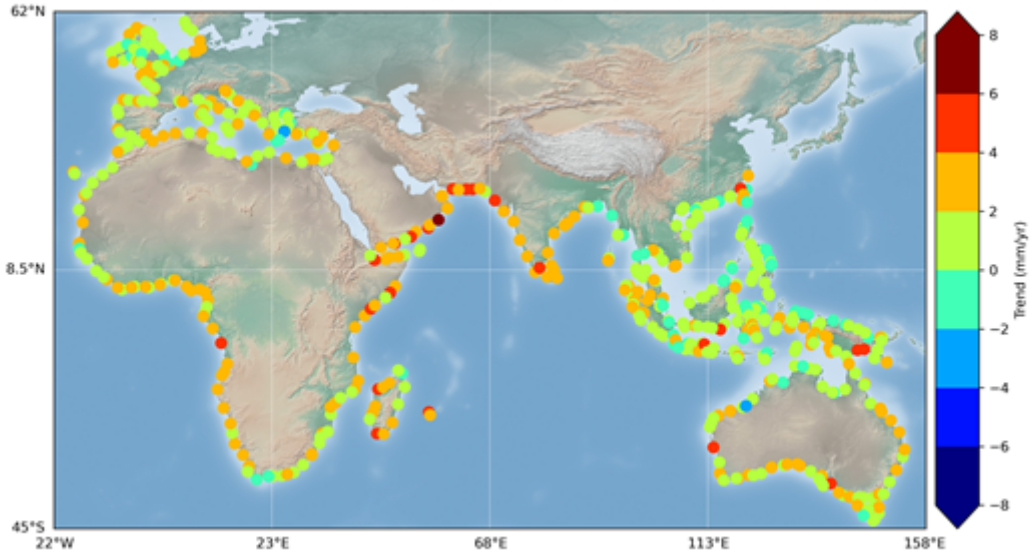

Figure 3*: Coastal trend estimates (mm/yr) over January 2002 to December 2019*

Compared to the version 1.1 product, the version 2.0 provides a larger number of valid trends in the 0-4 km band along the coasts (see Figure 2 and Figure 15 for comparison). This is illustrated in Figure 4 showing a map of sites where valid trend data are available within 4 km to the coast. Most cases are within 0-3 km. In the Mediterranean Sea and south Australia, the distance to the coast of the first valid trend is very small (better than 1-2 km).

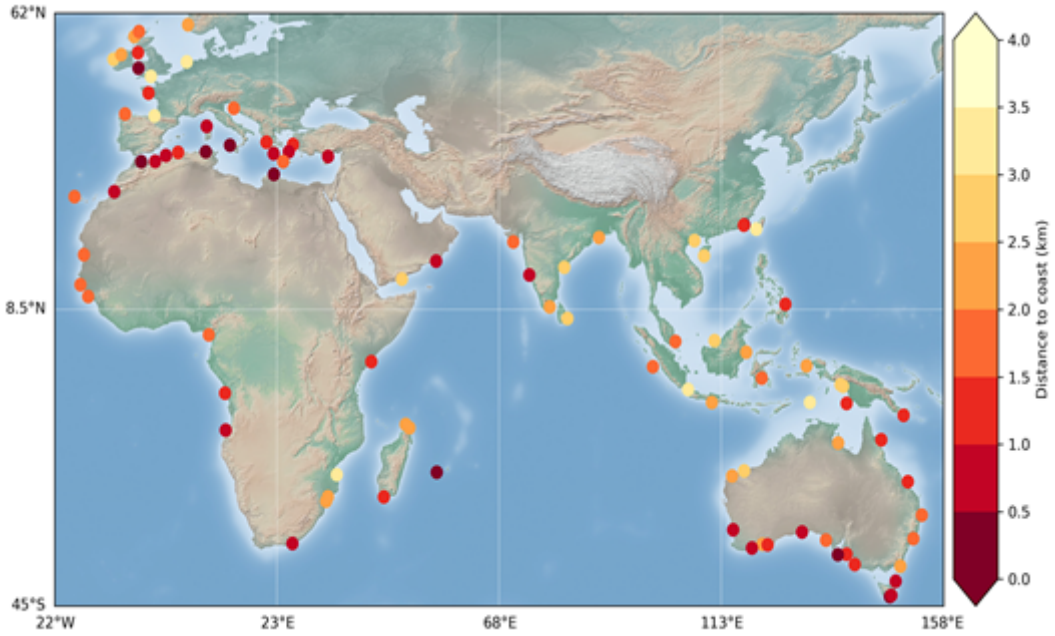

Figure 4*: Map of the sites where the distance to the coast of the first valid point is within 0-4 km to the coast.*

In Figure 5 are presented a few selected examples of coastal sea level trends against distance to the coast.

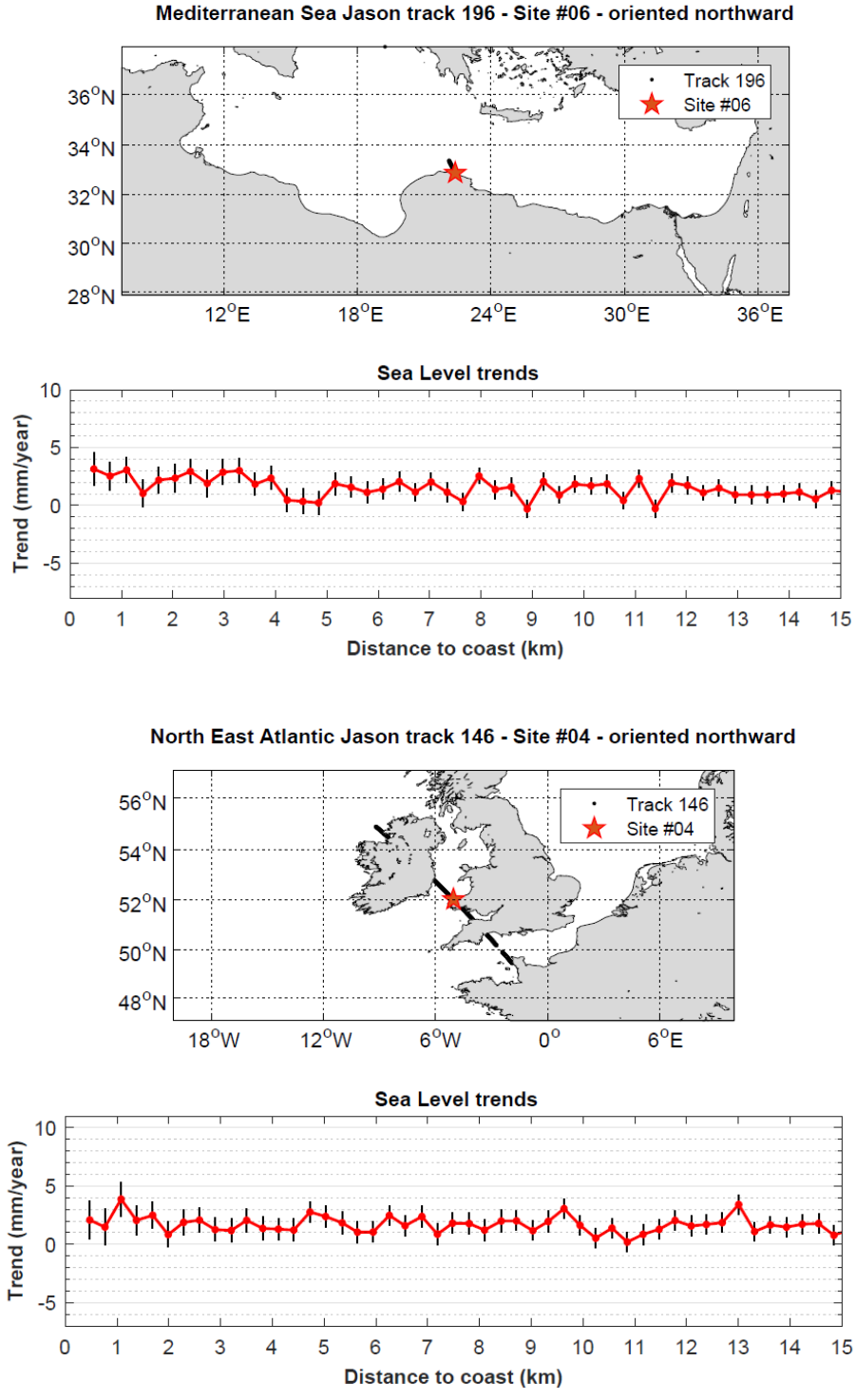

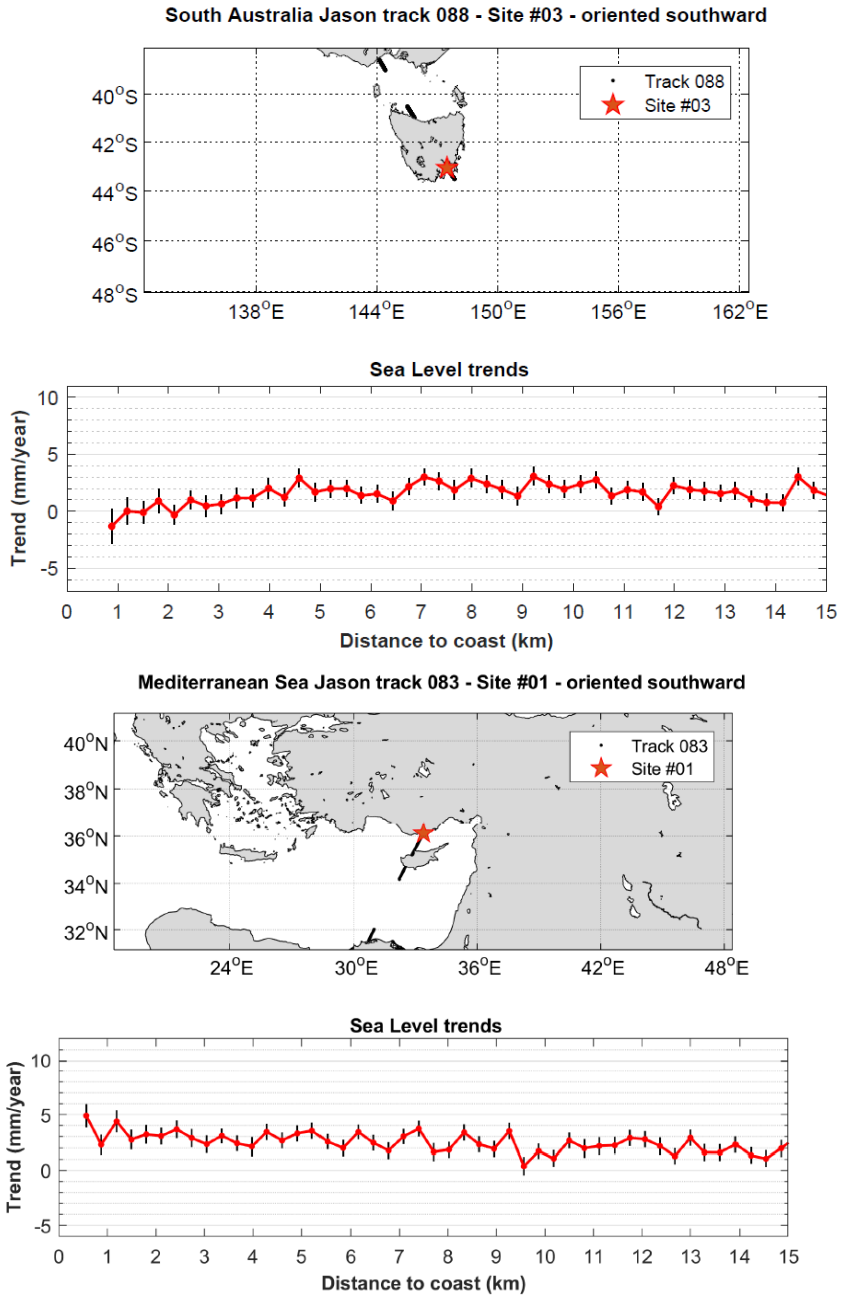

Figure 5*: Examples of coastal sea level trends (mm/yr) over 2002-2019 against distance to the coast.*

These new results show that in about 50% of the sites, the coastal trend does not differ by more than +/-1 mm/yr from the open ocean trend. The remaining 50% are almost equally shared by sites where the trend increases in the last 5 km to the coast

and sites where the trend decreases. This is illustrated in Figure 6 for the case where the closest distance to coast is > 4 km.

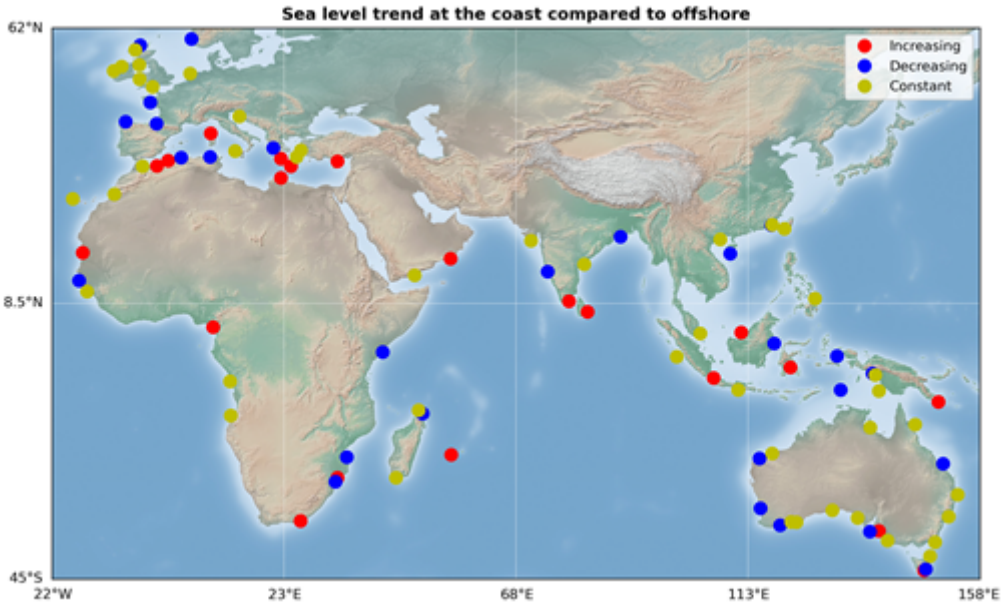

Figure 6*: map illustrating the behavior of coastal trends compared to offshore trends.*

The difference in trend behaviour from one site to another (that are in general distant by several km+) mostly depends on the differences in coastal processes that depend themselves on many different parameters (the coast morphology, bathymetry gradient, presence or not of a river estuary, etc). The understanding of these processes is not directly part of this project. This will require the analysis of available in situ coastal data and/or outputs of high resolution coastal ocean models.

Investigations are currently ongoing to estimate if the trend behavior is correlated with the bathymetry (hence the circulation). For that purpose, the Global Bathymetry dataset from Tozer et al. (2019) was used has been used. Its resolution is 15 arc second (e.g., ~500 m at equator).

Although this work is in progress, the conclusion is still uncertain. At most analyzed sites, no clear correlation between trend behavior and bathymetry is reported. Three examples are shown in Figure 7:

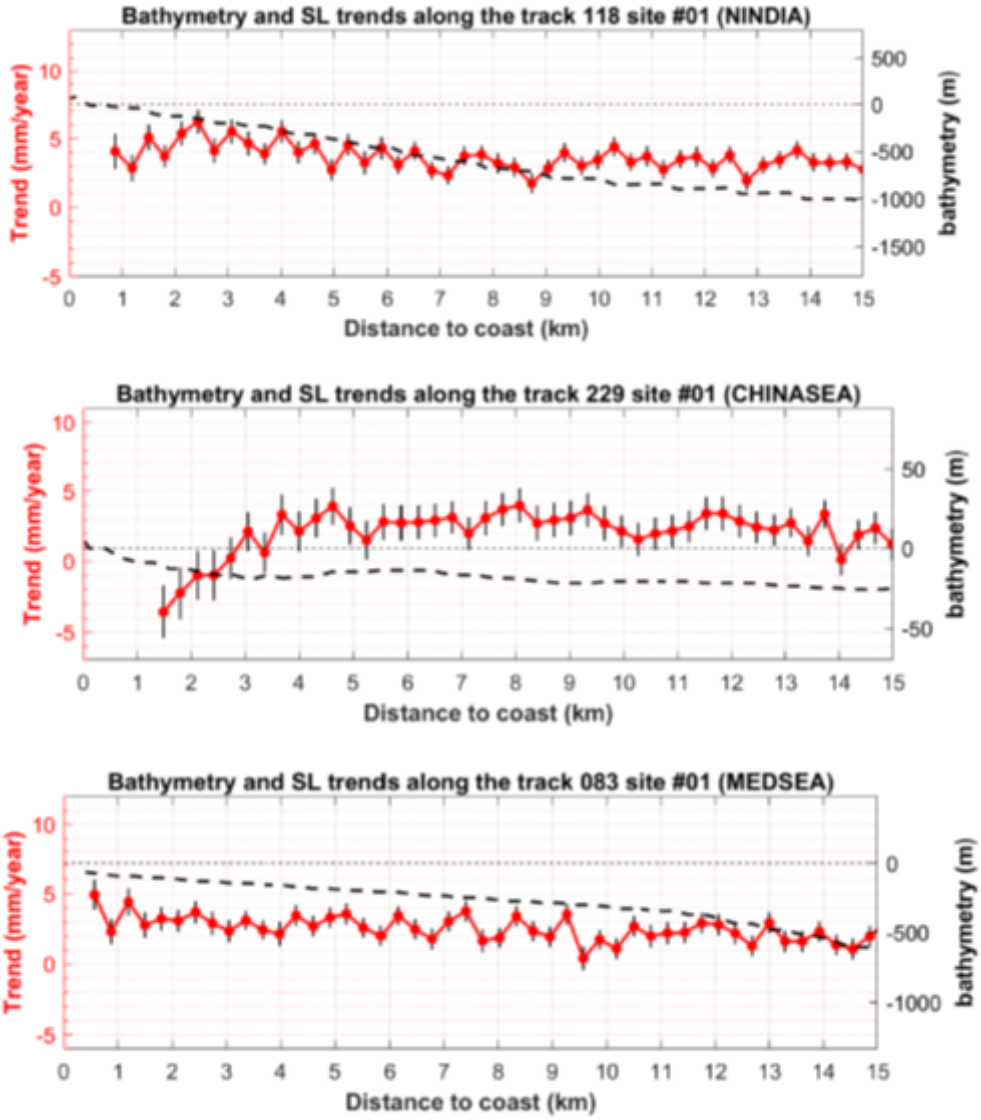

Figure 7*: Comparisons of sea level trends (red points) and associated errors (black vertical bars) and bathymetry (black thick dashed line) against distance to the coast.*

Other investigations concern the comparison between coastal sea level trends and open ocean steric sea level trends. This work is also in progress and will be reported later.

3. Validation of the coastal sea level products (NOC)

In this section we provide the results of a validation of the coastal sea level product (version 2.0) against tide gauge observations as well as a comparison of this product with the sea level product (version 1.1). Note that here we are validating the coastal sea level product (version 2.0) that has been developed with a focus on coastal

cities, while the validation that was conducted for version 1.1 as shown in Annex 1 (Section 5.3) used the raw data. Consequently, there are differences in the validation methodology. In particular, here we cannot use length scales to spatially average the altimetry data as we did for version 1.1 because the data for coastal cities only covers the first 20 km from the coast. Instead, the comparison is done in terms of point-level data as described below. This means that the correlations with tide gauge data shown here are likely to be lower than those shown in Annex1, but it is important to recognize that this is simply because spatiallly averaging as done for version 1.1 reduces the noise in the time series, in turn, leading to higher correlations. This effect of spatial averaging has been demonstrated in our *Scientific Data* paper. Another minor difference in methology is that here the comparison in terms of trends is restricted to tide gauge stations where there is a GPS station, while for version 1.1 we applied a GIA correction at such stations. The reason for this modification is that the fraction of vertical land movement unrelated to GIA can be very large at some stations and so correcting for GIA alone generally is not a good solution (Wöppelmann and Marcos, 2016).

3.1. Validation of coastal sea level product (version 2.0) against tide gauge data

The validation strategy is the same as described in our recent paper published in Scientific Data (The Climate Change Initiative Coastal Sea Level Team, 2020) for the coastal sea level product (version 1.1; see in annex 1 section 5). The tide gauge data consists of monthly mean values of sea level spanning the same period as the altimetry data and are obtained from the Revised Local Reference data archive of the Permanent Service for Mean Sea Level (http://www.psmsl.org/) (Holgate et al., 2013). To be consistent with the altimetry data, the same atmospheric correction that is applied to the altimetry data (i.e., MOG2D-G + inverse barometer) is also applied to the tide gauge data. The comparison between the two types of measurements is conducted in terms of sea-level variability (detrended and deseasoned monthly time series of sea level) and trends over the period from January 2002 to December 2018. In designing the validation strategy, a number of points merit consideration.

First, it is important to recognize that while the tide gauge data represent true monthly mean values, the altimetry monthly data are based on at most four measurements per month and so such data will be subject to sampling uncertainty due to variability at sub-monthly timescales. This sampling uncertainty will manifest as differences with the tide gauge observations, both in the variability and the trend. Exploratory analysis of this issue (see Annex) indicates that the effect of sampling uncertainty is fairly small when using three or more values per month, however it is more noticeable when using only one value per month and can degrade the correlation between the two otherwise identical time series, on average, from 1 to 0.7 and cause trend differences as large as 1.5 mm/yr. It is important to keep these effects in mind when interpreting the results of the validation against tide gauge data.

A second point to note is that, in general, altimetry measurements are not taken at tide gauge locations but at some ocean point nearby, and this spatial separation will inevitably lead to differences between the two types of data. The importance of

such differences will depend on the length scales of the sea-level signals around the tide gauges and can be significant. For this comparison, we first select the closest altimetry track to each tide gauge station and then, along this track, we select the altimetry time series showing the highest correlation with the tide gauge record. This altimetry time series is the one that we use in our comparison.

A third point to consider is that tide gauges measure sea level relative to the land on which they reside and so the measurements can be strongly affected by vertical land motion (VLM), particularly on long timescales. When comparing trends from altimetry and tide gauges it is important to account for this land contribution. Here, this is done by adjusting the tide gauge rates using Global Positioning System (GPS) vertical velocities. The GPS data consists of VLM rates from three different solutions (ULR, NGL, and JPL) and are obtained from SONEL (https://www.sonel.org). If there is a GPS station within 5 km of the tide gauge, then we use the rates from such station as our estimate of VLM (averaged over the various GPS solutions – ULR, NGL and JPL – available), otherwise we average the GPS rates over all GPS stations (and solutions) that are located within 50 km of the tide gauge. If there are no GPS stations within 50 km of the tide gauge, then we do not consider such tide gauge in the trend comparison.

The agreement between altimetry and the tide gauges in terms of trends is evaluated using fractional differences (FDs), which are defined as

$$\mathrm{FD} = |\tau_d|/(1.97 * \tau_d SE)$$

Where τ_d is the trend of the time series of the sea level differences between altimetry and the tide gauge, *SE* is the associated standard error and 1.97 is the critical value of the Student's t-distribution for the 95% confidence level. Hence, an FD value >1 means that, with 95% confidence, the two trends are statistically different. To be as rigorous as possible in the comparison of trends and obtain proper standard errors, we account for serial correlation in the estimation of the trends by using a regression model with first-order autoregressive errors. The model is analogous to that described by Chib (1993).

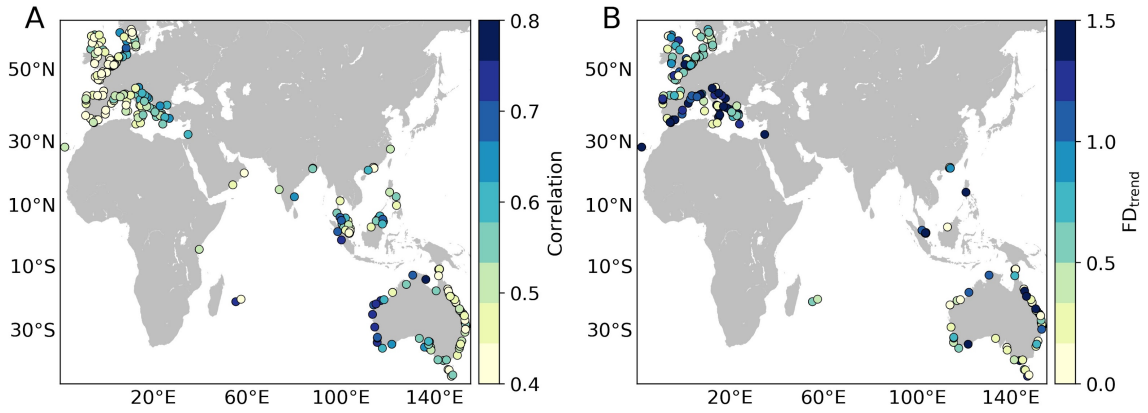

Figure 8. *Correlations (a) and trend FDs (b) for the comparison between altimetry and tide gauge observations. The correlations are for detrended and deseasoned monthly timeseries. Only tide gauges with a GPS station within 50 km are shown in (b).*

The average correlation between the altimetry and tide gauge time series across all tide gauge stations is 0.5, indicating an overall good match, but there are clear differences in agreement between regions (Fig.8a). These differences are most obvious along the Australian coastlines, where correlations are significantly higher along the western coast (>0.7) than on the eastern coast (~0.5). This is indicative of sea-level signals with shorter length scales along eastern Australia resulting in larger differences due to spatial separation, and thus it should not be interpreted as reflective of a difference in altimetric performance between the two coastlines. Sampling uncertainty due to variability at sub-monthly timescales present in the altimetry time series is also likely to play a role in explaining the relatively low correlations in some regions.

In regard to the trends (Fig. 8b), the median FD is 0.65 and FDs are <1 at 65% of the tide gauge stations, indicating that altimetry and tide gauge trends are in good agreement at the majority of stations. Again, there are regional differences such as the better agreement in western Australia compared to eastern Australia. This is again suggestive of shorter sea-level length scales along the eastern coast. There are 9 stations where FDs are >3, which reflects large trend differences. Such differences are likely due to local VLMs at the tide gauge stations that are not captured by the non-colocated GPS stations.

3.2. Sea level anomaly V2.0 Comparison with V1.1

For us to compare the SLA observations between V1.1 and V2.0 requires an exact match in the timestamp per observation or, at least, having the exact latitude and longitude coordinates. Unfortunately, this was not the case where both datasets had slightly different geographical coordinates and inconsistencies in the number of timestamp significant digits. In addition, V1.1 had some missing timestamp values that corresponded to valid SLA observations.

A time matching routine was applied to both datasets rounding the timestamps to 7 significant digits. The rounding of the V1.1 and V2.0 timestamps to 7 significant digits enables consistency between datasets for the SLA observation matchups to occur. A matching timestamp algorithm was applied to the West African region (Track 098, Figure 9). However, a timing problem was found where the V1.1 timestamp that corresponds to a matched V2.0 timestamp had some V1.1 latitude and longitude data laying outside the "common region", V2.0 (red dots lying outside the blue common region in Figure 9).

It was believed that this timing issue points towards the V1.1 dataset because some of the matched up V1.1 geographical coordinates lay outside the matched V2.0 region in sporadic points along the track (red dots). It was not clear that this issue occurs in the other geographical regions for V1.1, because both V1.1 and V2.0 had the same extracted regional geographical areas, unlike the West Africa region.

In more detail, an example of a miss-match is shown below in terms of latitude and longitude having the "same" timestamp, not rounded to 7 significant digits

Track 098 in the West African Region

Timestamp = 21599.00733503 v1.1, not rounded (days since 1950,1,1) this corresponds with lon -12.8501787185669 lat -5.6616792678833

Timestamp = 21599.0073349528 v2.0 not rounded (days since 1950,1,1) this corresponds with lon -13.0855321884155 lat -5.00958633422852

At this point in time, the "true" comparison between V1.1 and V2.0 unfortunately can't be done because of these issues. However, the SLA V2.1 is expected soon (2021), so the SLA MAD (Median Absolute Deviation) and trend comparison between V2.0 and V2.1 can be done for only the regions where both the datasets coincide.

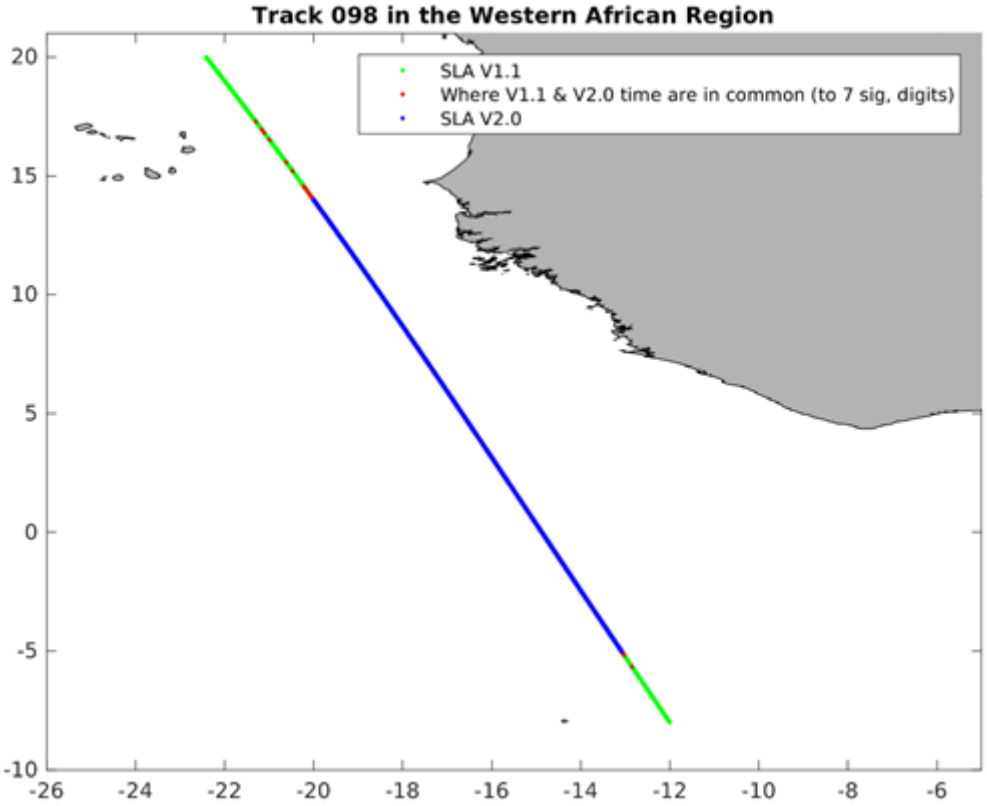

Figure 9: *A comparison between SLA V1.1 and V2.0 was carried out using the timestamp parameter as a common reference frame for both datasets. The green line represents the raw SLA v1.1 geographical coordinates along the Jason track 098. The blue line V2.0 is the region in common with V1.1. The red line/dots show the result of V1.1 coordinates that correspond with the same V2.0 timestamp (rounded to 7 significant digits).*

4. Sea level trend at Senetosa revisited

Recently, Gouzenes et al. (2020) showed that, over the June 2002-May 2018 time span, the sea level trend at Senetosa increases as the distance to the coast decreases. Gouzenes et al. (2020) showed that the trend increase in the last 3-4 km to the coast could not be explained either by erroneous trends in the geophysical corrections (i.e. sea state bias, wet tropospheric correction, dynamic atmospheric correction, ocean tide and ocean loading tide) applied to the altimetry data or by errors in the ALES retracking (use of the standard MLE4 retracker of Jason altimeter missions leads to the same trend bebavior). They concluded that some small-scale physical process may be responsible for the observed trend increase. They evaluated the contribution of waves but concluded that trend in waves is too small and active too close to the coast (last 1 km) to explain the reported trend increase.

We have revisited the Senetosa case using the extended coastal sea level time series (product 2.0), and examined another potential coastal process, i.e., the effect of sea water temperature T and salinity S changes close to the coast (Dieng et al., 2021). Because of the lack of in situ ocean parameters measurements, the high-resolution data from the MARS3D model were used. These model data cover the period January 2014 to December 2019 (unfortunately, the model output are not available prior January 2014). We interpolated the model T/S data along the 085/03 Jason track and computed the T/S trends as a function of depth and distance to the coast. Corresponding 2-dimensional T & S maps are shown in Fig.8a,b. We note an increase of the temperature trend with depth as the distance to the coast decreases. This indicates a thermocline deepening close to the coast (Fig.8a). An opposite effect is observed for the salinity trend with a decrease in salinity close to the coast (Fig.8b). These physical characteristics (increasing temperature trends and decreasing salinity trends) occur in the last ~4 km to the coast and are highly correlated with the bathymetry (see Fig.10a,b).

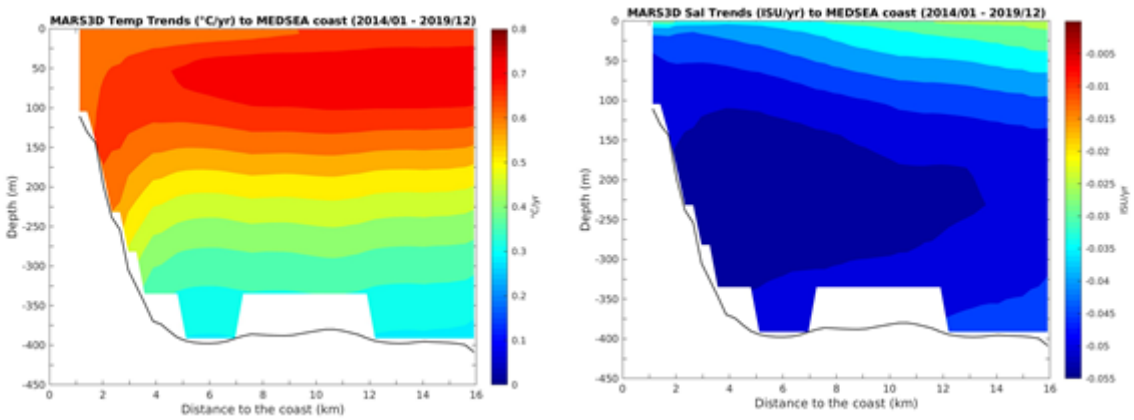

Figure 10*: (a) Temperature trend map, for site 085/03 near Senetosa. Based on the MARS3D model (calculated over the period January 2014 - December 2019) as a function of depth and distance at the coast along the altimeter track over the first 16 km of the coast. (b) same as (a) but for the salinity. The black curve is the bathymetric profile from the MARS3D model.*

We further computed separately the along-track thermosteric (T effect) and halosteric (S effect), integrating T/S data down to the seafloor. Fig.11 shows the thermosteric and halosteric sea level trends against distance to the coast, as well as their sum (steric component). The altimetry-based coastal sea level trend (over 2002-2019) is also superimposed.

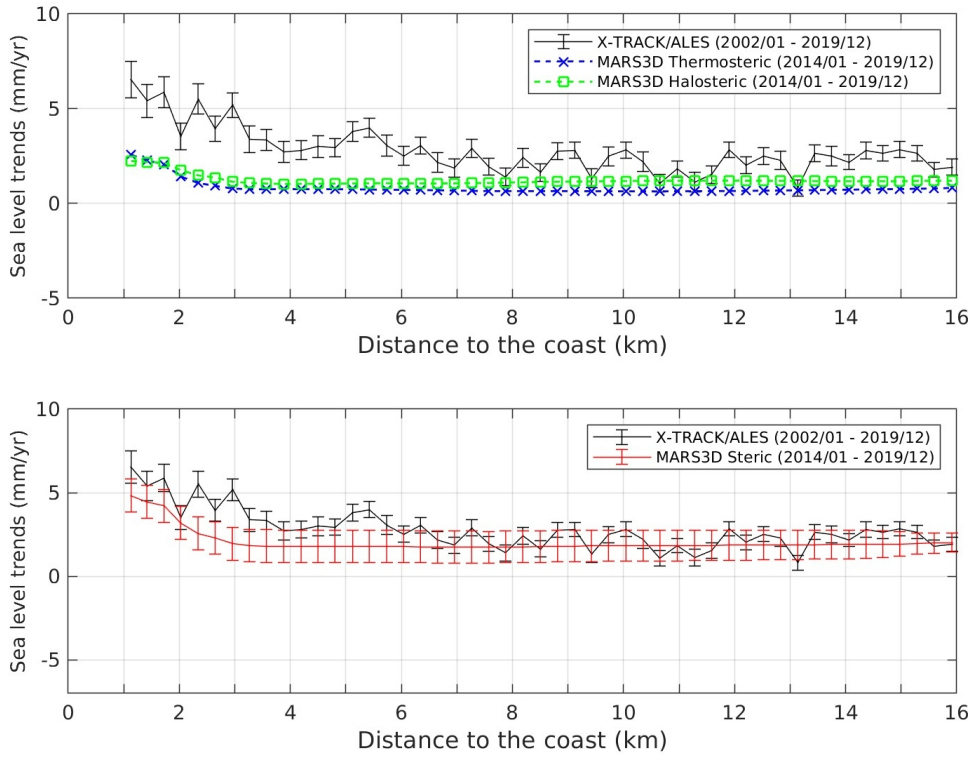

Figure 11. ***Upper panel : SLA trends at Senetosa (calculated over the period January 2002 - December 2019) (black curve) against distance to the coast compared to the thermosteric and halosteric trends (green and blue curves respectively). Lower panel : same as upper panel but with the total steric trends (red curve)***

Although observed and modeled coastal trends are not estimated over the same time span their respective behaviours against distance to the coast are very similar. Unfortunately, we cannot estimate reliable SLA trends over a time span as short as 6 years, i.e, 2014-2019, the results being too noisy.

This good agreement observed in Fig.8b between coastal sea level and steric trends may be fortuitous. Hence, the only conclusion we can draw so far is that, if the steric trend behaviour is a long-lived feature, change in T/S nearby Senetosa may be invoked to explain the SLA trend increase towards the coast. This could be eventually related to the presence of a wind-driven small-scale coastal current nearby the Senetosa shoreline, as shown in Gouzenes et al. (2020).

References:

The Climate Change Initiative Coastal Sea Level Team, Coastal sea level anomalies and associated trends from Jason satellite altimetry over 2002-2018, *Nature Scientific Data*, 7, 357, https://doi.org/10.1038/s41597-020-00694-w, 2020.

Dieng H.B., Cazenave A., Gouzenes Y. and Sow, A., Trends and inter-annual variability of coastal sea level in the Mediterranean Sea: Validation of high-resolution altimetry using tide gauges and models, in press, *Advances in Space Research*, 2021.

Tozer B., Sandwell D. Smith W. et al., Global Bathymetry and Topography at 15 Arc Sec: SRTM15+, Earth and Space Sciences, https://doi.org/10.1029/2019EA000658, 2019.

5. ANNEX 1: Presentation of the initial v1.1 coastal sea level trends

5.1. Processing methodology

The reprocessing method consists of: (1) using an adapted retracking methodology to estimate the altimeter range from waveforms collected in the coastal zone, (2) using improved geophysical corrections, and (3) applying a strict data editing procedure adapted to coastal ocean conditions. The approach has been applied to the high frequency (20-Hz, corresponding to a ground separation of ~300 m between two estimates) along-track measurements from the Low Resolution Mode of the Jason-1, Jason-2 and Jason-3 missions (the output products have been produced with this 20-Hz along-track resolution). For each satellite track, the sea level data of each mission have been combined into a single record over the study period, and further expressed in terms of sea level anomalies located along a theoretical mean reference track. At all 20 Hz points along the track, the original sea level anomalies at 10-day interval have been further averaged on a monthly basis and sea level trends over the whole study period have been computed. For more details, see the Climate Change Initiative Coastal Sea Level Team, 2020 and the Product User Guide (https://climate.esa.int/en/projects/sea-level/key-documents/, Tech. Coastal SL).

From the 10-day X-TRACK/ALES sea level anomalies (SLAs), we constructed another edited product called 'Coastal Sea Level Product 2' that not only includes SLA time series (expressed as monthly averages), at each 20-Hz point along a track portion of 20 km from the coast, but also sea level trends and associated standard errors. This 'Coastal Sea Level Product 2' contains a much smaller number of track portions than the original data set because based on a severe data selection, largely based on trend estimates (see below). The product includes monthly SLAs, simply computed by averaging available 10-day data (the monthly SLAs are based on a maximum of 4 values but sometimes only 2 or 1 value are available in the monthly interval). At each along-track 20-Hz point from 20 km offshore to the coast, annual and semi-annual signals were removed by fitting sinusoidal functions to the SLA time series. An editing was further applied by computing the mean of the deseasonalized and detrended SLA time series, and removing outliers located outside a 2-sigma threshold around the root mean squares of the time series. After re introducing the initial trend, a new trend and its associated 1-sigma formal error were estimated through a least-squares fit of a linear function to the edited SLA time series. Note that we do not correct the SLA time series for the regional contribution of Glacial Isostatic Adjustment. Such a correction is small (<1 mm/yr) and can be further removed from the estimated trends by the users.

The criteria considered for the selection of the monthly SLAs plus trends of the Coastal Sea Level Product 2 are listed below:

- Number of valid data of the SLA time series at each 20-Hz points (missing data <50%)

- Distribution of the valid data as uniform as possible across the three Jason missions. In a number of cases, Jason-1 data were much less numerous than the Jason-2 data. The corresponding SLA time series were then discarded.
- Trend values in the range –15 mm/yr to +15 mm/yr
- Standard errors on trends < 2 mm/yr.
- Continuity of trend values between successive 20 Hz points. Too abrupt changes in trends over very short distances were considered as spurious and the corresponding point was removed. This mostly occurred close to the coast but sometimes, at a larger distance from the coast.

With this selection approach, we discarded a large number of along-track 20-Hz points considered as not accurate enough to compute reliable trends. For the v1.0 coastal trends dataset, this led us to retain only 429 track portions from the initial set of 628 original track portions. We further identified them by a coastal site where the satellite track crosses land. The selected sites are named by the region and the track number to which they belong and by the site number on the track, going from north to south.

5.2. Statistics on coastal sea level trends (version 1.1)

In this section, we present statistics on coastal sea level trends and associated trend errors, as well on distances to the coast of the first valid point for the 429 selected sites. These results are shown in the form of histograms. For coastal trends and associated errors, separate histograms are provided for ascending and descending satellite tracks, as well as for 'sea to land' and 'land to sea' flying directions. Similarly, histograms of closest distance to the coast of the first valid point are presented for ascending and descending satellite tracks, as well as for 'sea to land' and 'land to sea' flying directions. In all cases, this is done for all six regions together and for each region individually. Results are presented in Figure 12 and Figure 13 for all six coastal zones.

The histograms shown in Figure 12 display no differences between ascending and descending tracks in terms of trends distribution. Although it has to be noted that the sites where the track crosses land are different for ascending and descending tracks, the distributions looks quite similar in both cases and mean trend values are on the same order of magnitude within 0.1 mm/yr. The mean value for all tracks amount to 2.6 mm/yr. Note that this trend value is not GIA-corrected.

The mean and median trend errors are also similar for ascending and descending tracks, and on the order of 1.1 mm/yr. Note that there is no trend error larger than 2 mm/yr, a consequence of one of our selection criteria.

In Figure 13 are shown the distributions of the closest distance to the coast (first valid point) for the same configurations as Figure 12. Again little difference is observed between ascending and descending tracks, with a mean distance of 3.5 km for all sites. On the other hand, we note better performance for the sea to land configuration (mean value of 3.2 km, more sites with closest distance to coast < 2 km) than the land to sea configuration.

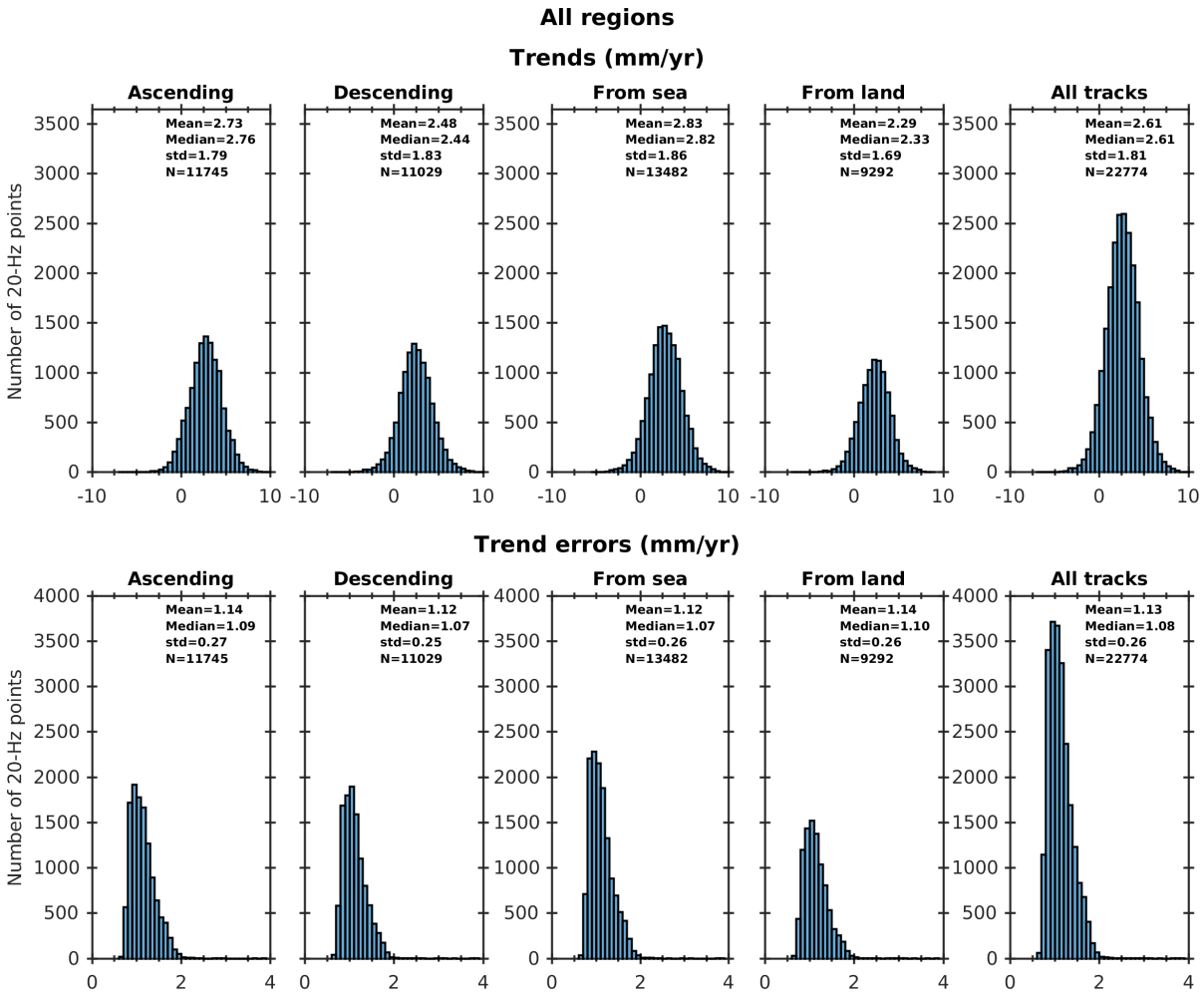

Figure 12: *Histograms of trends (mm/yr) for ascending, descending, sea to land, land to sea and all tracks (upper panel); Histograms of associated trend errors (mm/yr) (lower panel).*

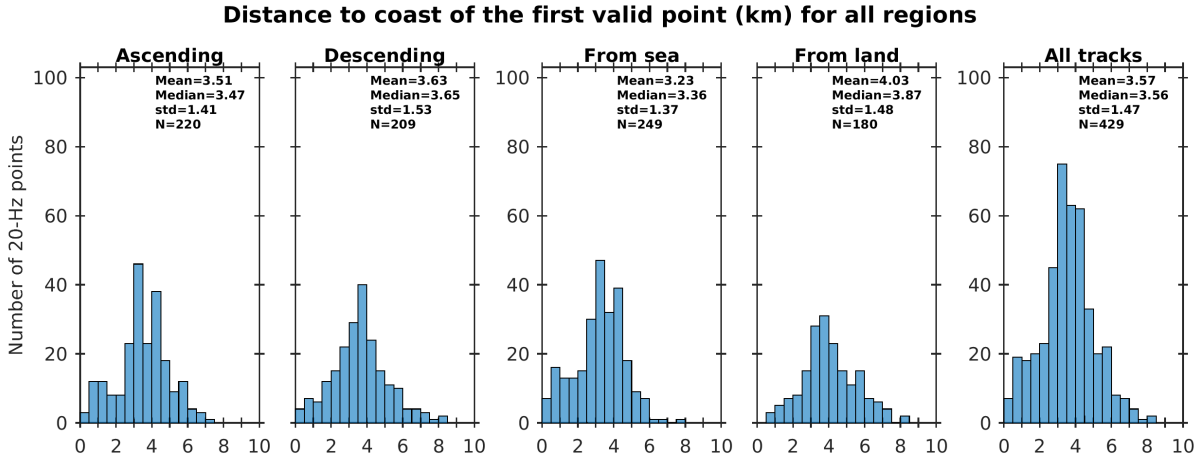

Figure 13. *All regions: Histograms of distance to coast of the first valid point (km) for ascending, descending, sea to land, land to sea and all tracks.*

Similar histograms for individual regions (not shown) display some differences from one region to another. In the **Mediterranean Sea**, 70 sites are selected. Their mean coastal trend is 1.9 +/-1.0 mm/yr. No difference is noted between ascending and descending tracks. There is a smaller amount of land to sea configurations in the selected sites, with slightly smaller coastal trends (1.7 +/- 1. mm/yr) than in the sea to land case (coastal trends of 2. +/- 1. mm/yr). The distances of the first valid point to the coast are spread from < 1 km to > 5 km. The mean distance is in the 3-4 km range but a larger number of cases fall within less than 2 km from the coast.

In **the northeast Atlantic region**, 44 sites are selected. The mean trend is 2.0 +/- 1.2 mm/yr. Only slight difference is observed between ascending (1.85 +/- 1.2 mm/yr) and descending tracks (2.05 +/- 1.2 mm/yr). Five time more measurement points are seen for the sea to land configuration than the land to sea one. The mean distance of the closest valid point is 3.5 km, with only few cases < 2 km and most of the distribution lying between 2 km and 4 km.

26 sites only are selected along the **Western Africa region**. The mean rate of coastal sea level rise is 2.15 +/- 0.9 mm/yr. Along ascending tracks, the mean trend is 2.0 +/- 0.9 mm/yr while it is only 1.35 +/- 0.9 mm/yr along descending tracks. But the latter concerns a much smaller number of measurement points. We also observe more sea to land cases than land to sea, due to the particular configuration of the African coast and Jason tracks. On average, the closest distance to coast distribution is in the 2-4 km range, with most of the cases included between 3 and 4 km to the coast. In the northern Indian Ocean region, 57 sites have been selected. The average distance to coast of the first valid point lies in the 3-4 km range but we observe a large spread from < 1 km to > 5-6 km from the coast. The mean trend is 3.5 +/- 1. mm/yr, with no noticeable difference between ascending and descending tracks nor between sea to land and land to sea directions.

The Southeast Asia region displays the largest number of selected sites (177), with a mean trend of 2.7 +/- 1.2 mm/yr. As for the north Indian Ocean region, no significant difference is seen between ascending and descending tracks nor between sea to land and land to sea directions. The mean distance of the closest valid point is 3.8 km, with a maximum of the distribution between 3 km and 4 km.

Finally, 55 sites are selected **around Australia**. The mean trend is 3.2 +/- 1.2 mm/yr. In this region, several sites display sea level trends of 5 mm/yr or larger. We note more valid points for ascending than descending tracks. The mean value of the closest distance to coast is 3.3 km, with a more or less uniform distribution between the coast and 6 km offshore.

A map of coastal trends (averaged over 2 km along-track from the first valid point) is shown in Figure 14. The figure indicates that at a significant number of sites, over the study period, the coastal sea level rise is in general positive (with a few exceptions), with values as high as 4-5 mm/yr in some regions. This is particularly

the case in the northern and eastern parts of the Indian ocean (around Indonesia for the latter).

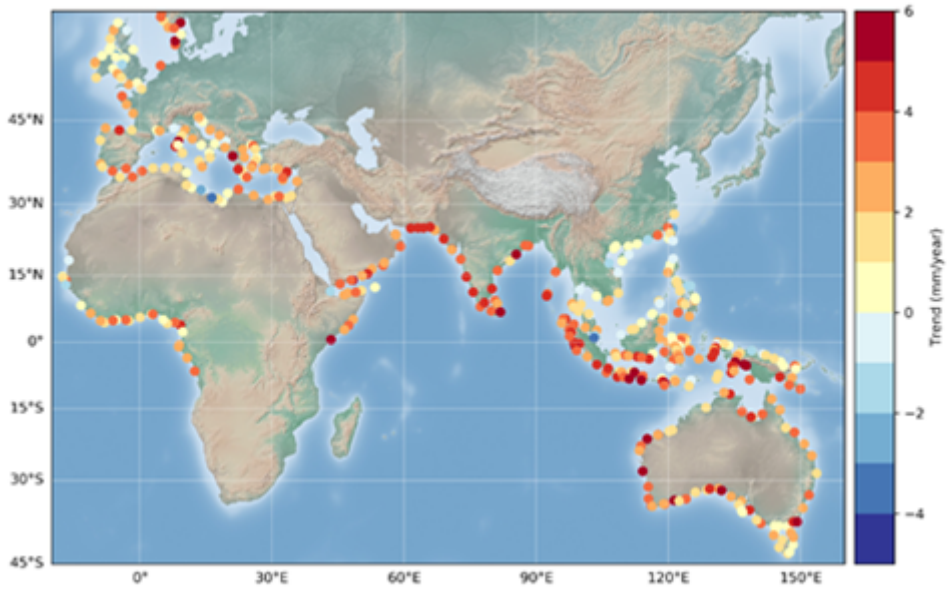

Figure 14. ***Coastal sea level trends (mm/yr) at the first valid point from the coast at the 429 selected sites.***

In Figure 15 is shown a map of the distance to coast of the first valid point.

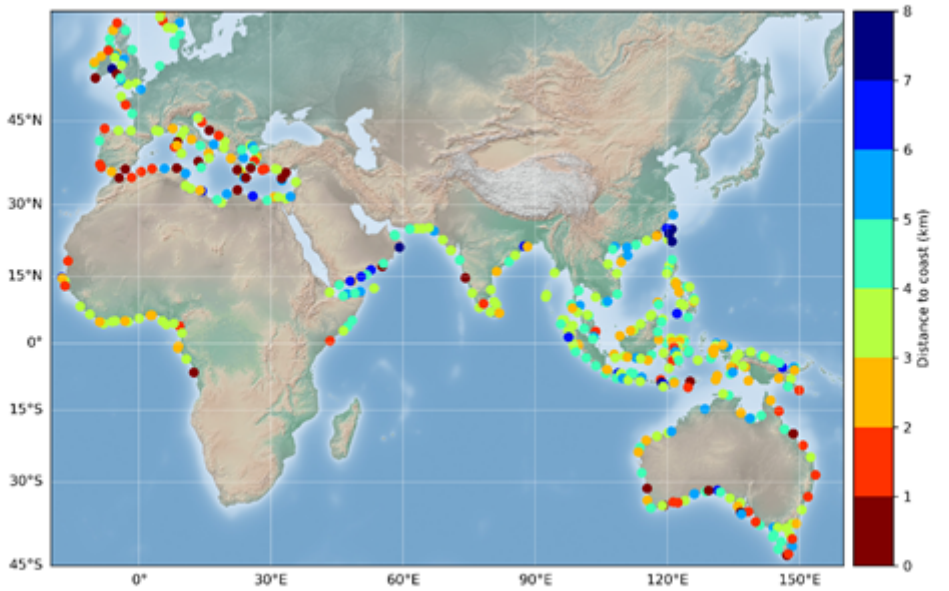

Figure 15*: Map of the closest distance (km) to the coast of the first valid point from the coast at the 429 selected sites.*

Figure 15 shows that in most regions, the distance to the coast of the first valid point in the 3-4 km range, but as discussed above, the closest distance to the coast can be <2 km, particularly in the Mediterranean Sea and around Australia.

In order to investigate whether the coastal trends shown in Figure 14 differ from open ocean trends, the differences in sea level trends between an along-track portion of 2 km from the closest valid point to the coast and the 14-16 km average, offshore, have been computed. These are shown in Figure 16.

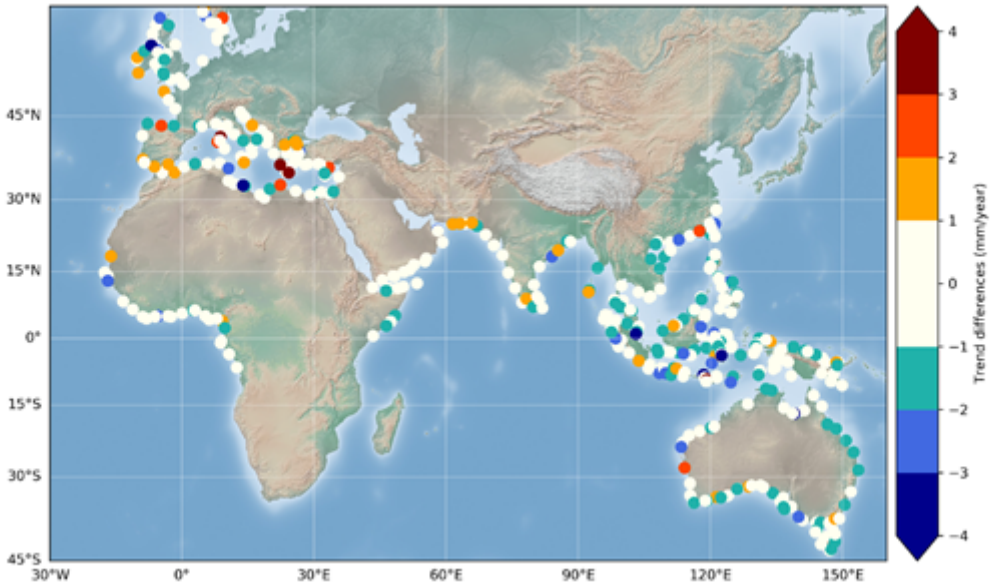

Figure 16. ***Differences in sea level trends between an along-track band of 2 km from the closest valid point to the coast and the 14-16 km average, offshore. White points correspond to no significant differences (within +1/-1 mm/yr) between open ocean and coast. Orange-red/blue dots correspond to coastal trend increase/decrease at the coast.***

The trend difference map presented in Figure 16 shows an unexpected result: In most places, no significant difference (within +/-1 mm/yr) is noticed between the open ocean and the coastal zone. However, this is not always true. At a few sites, we observe a larger trend close to the coast than offshore, but with the exception of 3 sites in the Mediterranean Sea and one site in Australia, the increase is modest, of 1-2 mm/yr only, and possibly not significant in view of the trend uncertainties. In a number of cases, we note a decrease in trend as the distance to the coast decreases (blue points on the map). But here again just a few cases may be significant. Although it had been expected that coastal processes may cause some discrepancy in coastal sea level trends compared to the open ocean (e.g., Woodworth et al., 2019), the results presented here seem to contradict this hypothesis. If confirmed by further studies, **an important consequence of this observation is that it would be possible to extrapolate regional sea level trends computed by classical altimetry missions.**

In Figure 17 below are shown for each region, maps of sites where the trend at the coast differs by more than 1.5 mm/yr from offshore.

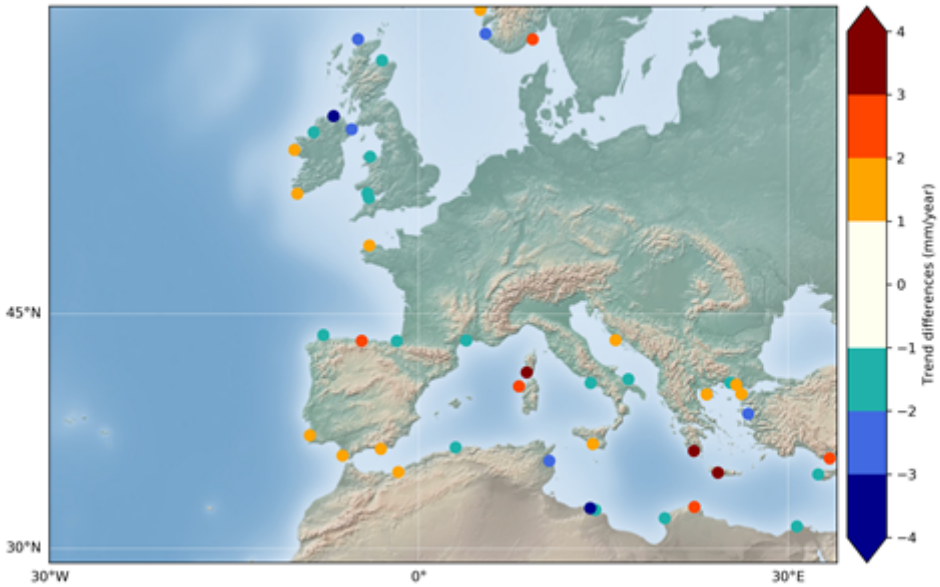

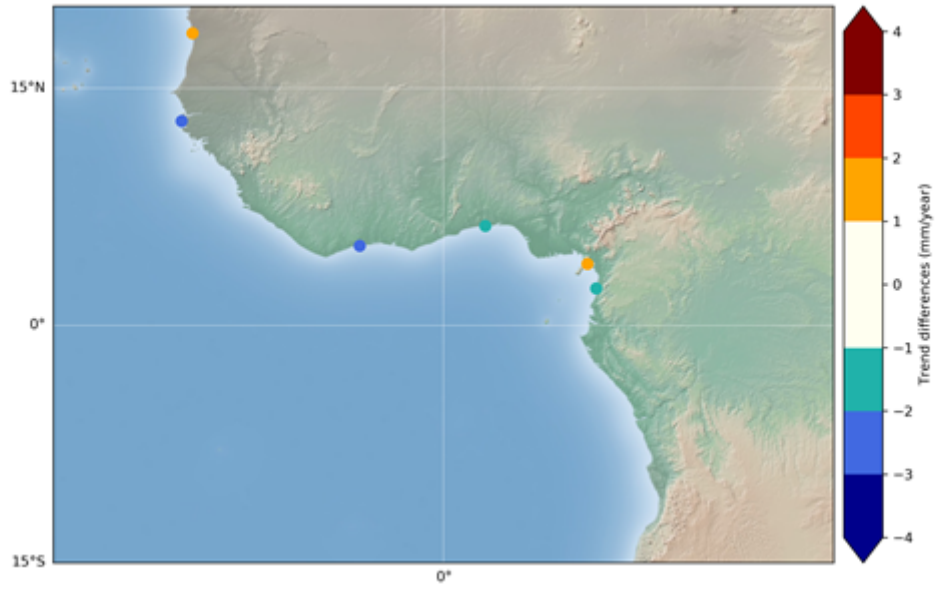

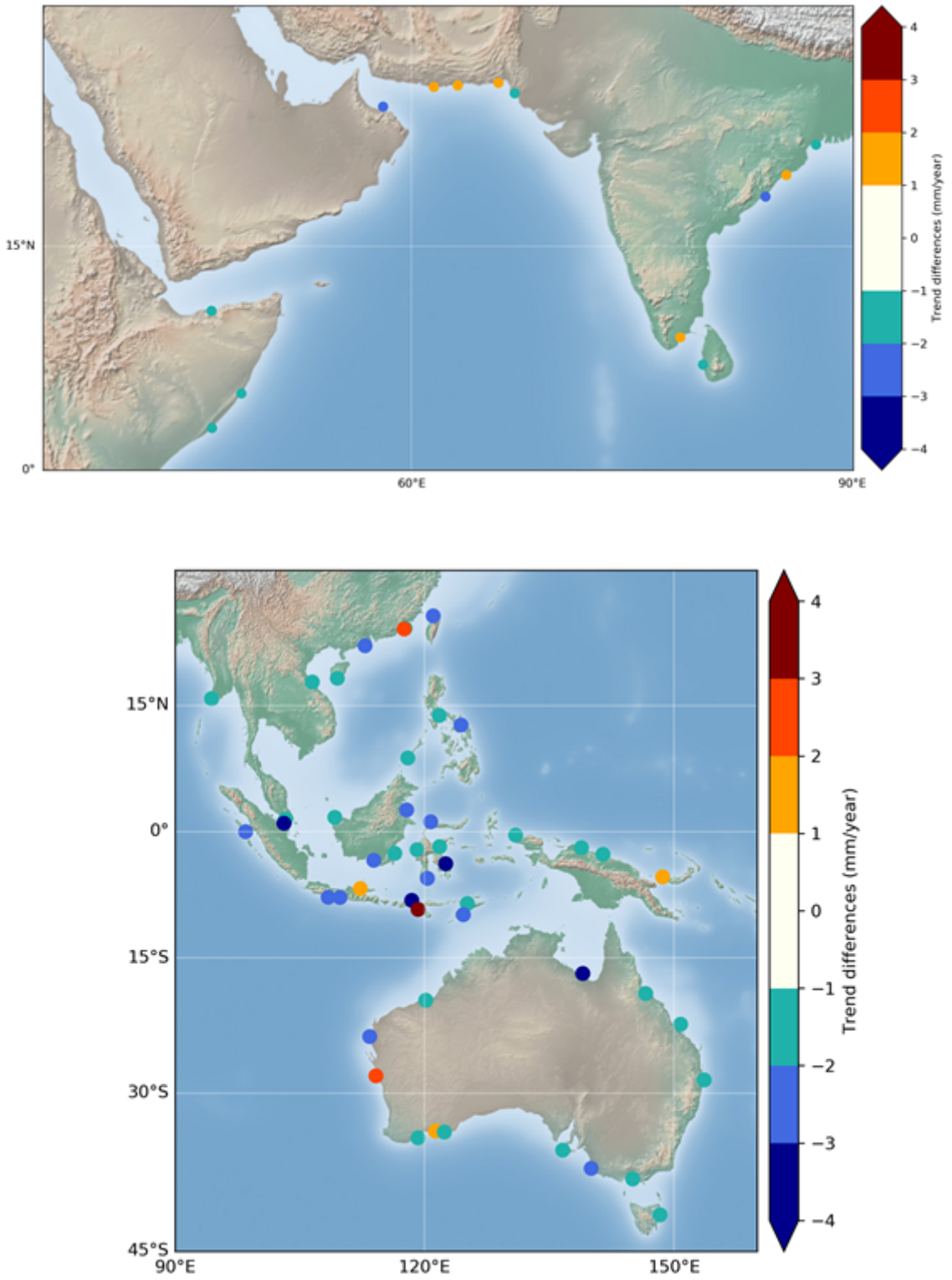

Figure 17: Map of sites where the trend at the coast differs from 1.5 mm/yr from offshore (Northeast Atlantic and Mediterranean Sea, Western Africa, North Indian Ocean and Southeast Asia and Australia)

5.3. Validation with tide gauges (version 1.1)

5.3.1. Data

This section presents the validation of the SL_cci+ coastal sea level product (v1.1) against tide gauge data in six regions, namely the Northeast Atlantic Ocean, the Mediterranean Sea, the Western African coast, the North Indian Ocean, Southeast Asia, and Australia. The altimetry dataset covers the period from January 2002 to May 2018. The tide gauge data used here consists of monthly mean values of sea level spanning the same period as the altimetry data and are obtained from the Revised Local Reference data archive of the Permanent Service for Mean Sea Level (http://www.psmsl.org/) (Holgate et al., 2013). To be consistent with the altimetry data, the dynamic atmospheric correction (DAC) is applied to the tide gauge data.

If the sea floor at the location of a tide gauge does not move vertically, then collocated altimetry and tide gauge measurements will provide observations of the same quantity. While generally the assumption of no vertical land motion (VLM) is a reasonable one when the focus is on inter-annual or shorter timescales, it does not hold on long timescales. In particular, accounting for VLM is essential for a proper comparison between altimetry and tide gauge data in terms of trends. Hence, here we use GPS vertical velocities to adjust the tide gauge trends for VLM wherever a GPS station is near the tide gauge (the criteria for selecting GPS stations is described later in Section 5.3.3), otherwise we adjust the tide gauge trends only for the Glacial Isostatic Adjustment (GIA) contribution to crustal uplift. The GPS data consists of VLM rates from three different solutions (ULR, NGL, and JPL) and are obtained from SONEL (https://www.sonel.org), whereas the GIA data are estimates from the ICE-5G v1.3 model (Peltier 2004).

5.3.2. Important considerations

In validating altimetry observations against monthly tide gauge data, it is important to recognize that while the tide gauge data from the PSMSL represent true monthly mean values (they are computed as the arithmetic average of the daily mean sea level values in each month), the along-track altimetry data consists of at most four measurements per month at any particular location and thus altimetry monthly means will necessarily be subject to sampling uncertainty due to variability at sub-monthly timescales. This sampling uncertainty will manifest as differences with the tide gauge observations, both in the variability and the trend. We will show later that by merging altimetry data from different tracks based on the characteristic spatial length scales of the sea level signals around the tide gauges allows us to use more values to compute monthly averages, thus alleviating the issue of sampling uncertainty and enabling a more appropriate assessment of the altimetry data. We also note that because the altimetry monthly values might be based on a different number of values each month, the variance of the timeseries might not be constant; an issue termed heteroskedasticity in statistics. If large, heteroskedasticity can lead to biased standard errors in ordinary least squares models, but it does not cause the regression coefficient estimates (e.g., trends) to be biased.

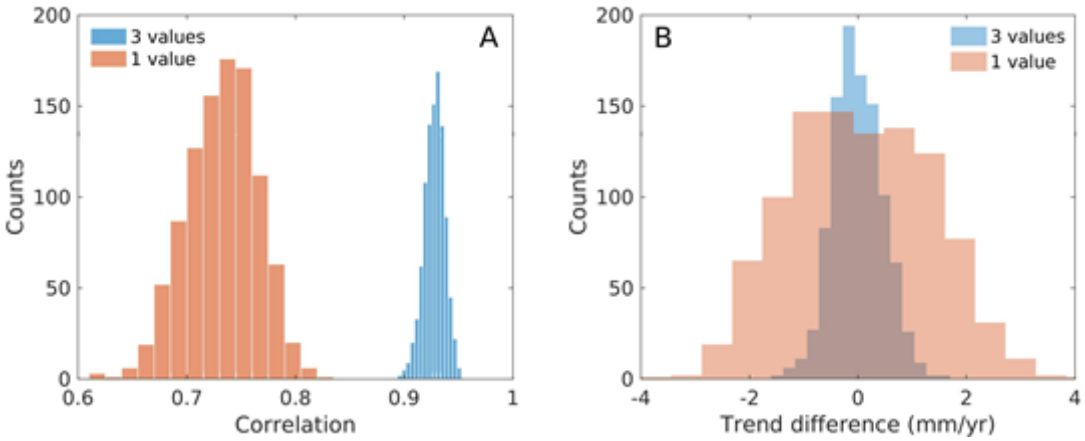

Figure 18: (A) correlation of 3-value and 1-value monthly timeseries with the true monthly means. (B) Difference in trend estimates from 3-value and 1-value monthly timeseries relative to the trend from the true monthly means.

5.3.3. Validation procedure

In designing the validation strategy, a number of points merit consideration. First, it is important to recognize that variability and trends in sea-level are generally driven by different mechanisms and hence have different spatial length scales; while the former is largely associated with internal variability in the ocean-atmosphere

system, trends are primarily due to ocean warming and land-ice melting. This implies that the agreement between altimetry observations and tide gauge data might be different depending on the temporal scales of variability that one is looking at. In turn this means that a good agreement in terms of trend does not imply the same for the variability and vice versa, and hence the validation needs to be conducted specifically for each temporal component. Here, we will compare the two types of datasets in terms of the sea-level annual cycle (annual amplitudes), intra-annual variability (correlations), and trends over the period from January 2002 to May 2018. As part of the processing of the altimetry data, we remove values of sea-level anomalies beyond both 2 m and 3 standard deviations (over the period 2002-2018); this is the only editing of the altimetry data performed here involving outlier rejection.

A second point to consider is that, in general, altimetry measurements are not taken at the tide gauge locations but at some ocean point nearby, and this spatial separation will inevitably lead to differences between the two types of data. The importance of such differences will necessarily depend on the length scales of the sea-level signals around the tide gauges. Hence, to minimize the impact of errors due to spatial separation on our validation, we estimate coherence length scales at each tide gauge and then consider only altimetry data that falls within these length scales around the tide gauges. At each tide gauge, the characteristic length scale is calculated by first correlating the deseasoned and detrended sea-level from the tide gauge record with that from along-track altimetry, and then fitting a Matérn function (Rasmussen and Williams, 2006) to the vector of correlations as a function of distance to the tide gauge. Length scales are computed separately for each track and so different tracks might have different length scales. Note that by convention the length scale is the distance at which the correlation with the tide gauge data is 0.4, hence only tracks that have data with a correlation above 0.4 are considered. Using only altimetry data within a length scale from the tide gauge can reduce differences due to spatial separation. In addition, if more than one altimetry track falls within the estimated length scale, this allows us to merge the data and compute monthly timeseries based on many more than 3 or 4 values, alleviating the issue of sampling uncertainty. For example, if two tracks fall within the length scale, we are able to compute monthly means using up to 8 values per month, if there are three tracks then we can use up to 12 values per month, and so on. We construct two types of altimetry timeseries at each tide gauge: 1) we merge all the altimetry data from all tracks that fall within the characteristic length scale into one single ‘best’ altimetry timeseries; and 2) we bin and merge the altimetry data according to distances to the coast at intervals of one kilometre, thus generating one altimetry timeseries for each distance to the coast. Timeseries 2) enables us to assess the performance of the altimetry data as a function of distance to the coast.

A third point to note is that the sea level from tide gauge records can be strongly affected by VLM. Hence, when comparing rates of sea-level rise from altimetry and tide gauges it is important to account for this land contribution. Here, this is done by adjusting the tide gauge rates using GPS vertical velocities as follows. If there is a GPS station within 5 km of the tide gauge, then we use the rates from the closer GPS station as our estimate of VLM at the corresponding tide gauge (averaged over the various solutions – ULR, NGL and JPL – available), otherwise we average the GPS

rates over all GPS stations (and solutions) that are located within 50 km of the tide gauge. If there are no GPS stations within 50 km of the tide gauge, the tide gauge sea-level rates are adjusted only using the GIA contribution to crustal uplift.

The agreement between altimetry and the tide gauges in terms of trends is evaluated using fractional differences (FDs), which are defined as

$$\mathrm{FD} = |\tau_d|/(1.97 * \tau_d SE)$$

where τ_d is the trend of the time series of the sea level differences between altimetry and the tide gauge, *SE* is the associated standard error and 1.97 is the critical value of the Student's t-distribution for the 95% confidence level. Hence, an FD value >1 means that, with 95% confidence, the two trends are statistically different. To be as rigorous as possible in the comparison of trends and obtain proper standard errors, we account for serial correlation in the estimation of the trends by using a regression model with first-order autoregressive errors. The model is analogous to that described by Chib (1993). In the presence of strong serial correlation, this model is more efficient than ordinary least squares (i.e., trend estimates are more precise) and yields more proper standard errors.

5.3.4. Results

Correlations

The correlation between detrended, deseasoned sea level from tide gauge records and satellite altimetry (the 'best' timeseries computed as described in Section 5.3.3) is shown for the six study regions in Figure 19. The correlations are fairly uniform across both tide gauge stations and regions with a mean value of ~0.77, indicating an overall good match between the two types of measurement. While, in general, differences in correlation tend to be small across stations, a clear spatial structure is noticeable in some of the regions. This is most obvious along the Australian coastlines (Figure 19F), where correlations are higher along the western coast compared to the eastern coast. This is indicative of sea-level signals with longer length scales along western Australia and should not be interpreted as reflecting a difference in altimetric performance between the two distinct coastlines.

The correlations shown in Figure 19 are based on altimetric timeseries that are formed by merging all the altimetry data that fall within a characteristic length scale at each tide gauge (what we call 'best' altimetry time series). However, we can further group the altimetry data in terms of distance to the coast and this can be used to obtain a measure of the closest location to the coast at which the altimeter performance remains high. Here performance is measured in terms of correlation. We find that at most locations the closest we can get to the coast before correlations start to drop is between 2 and 6 km, with a mean value of 4 km (Figure 20). There are very few locations where we can get closer than 1 km without seeing a substantial decrease in correlation between the tide gauge and altimetry data.

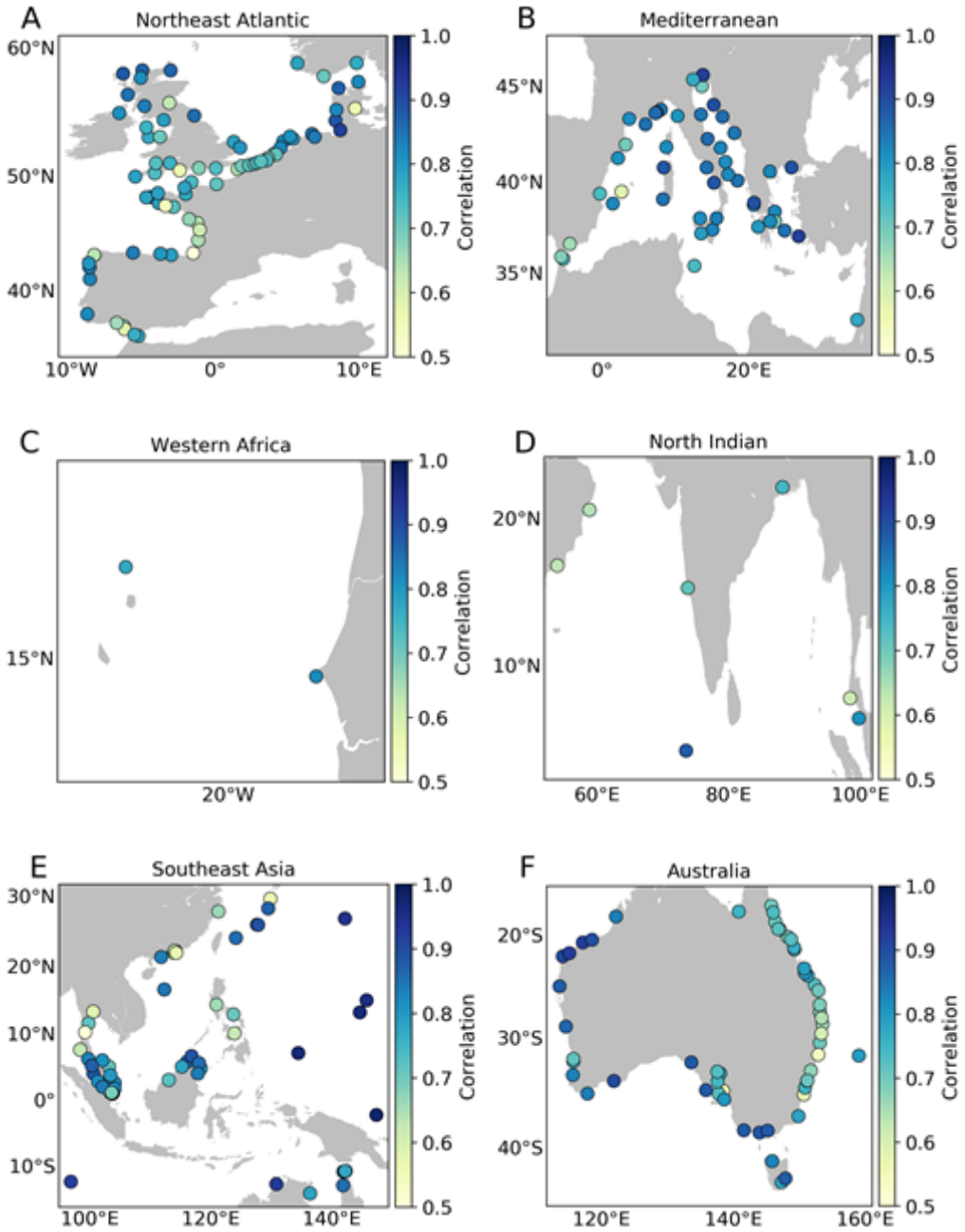

Figure 19: Correlation of detrended, deseasoned sea level from tide gauge records and satellite altimetry (the 'best' timeseries computed as described in Section 5.3.3) in (A) the Northeast Atlantic Ocean, (B) the Mediterranean Sea, (C) the Western African coast, (D) the North Indian Ocean, (E) Southeast Asian, and (F) Australia.

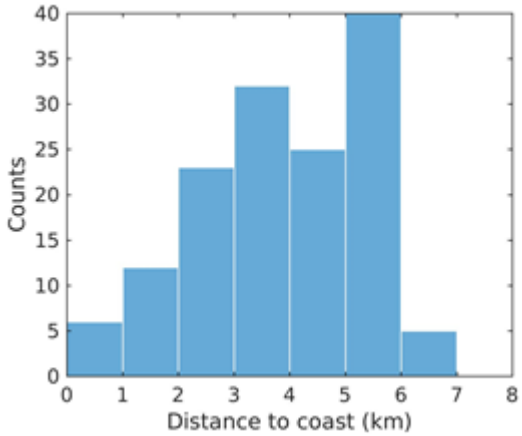

Figure 20: Histogram showing the closest distance to coast where the correlation between the tide gauge and altimetry data remains consistent with the correlation at more distant locations.

Annual amplitude

At many coastal locations the sea-level annual cycle is the most energetic signal outside the tidal frequency band and so a comparison between the altimetry and tide gauge data in terms of this cycle provides a first-order assessment of the data and might highlight the existence of gross errors. Figure 21 shows the FDs for the amplitude of the sea-level annual cycle. The agreement between the two types of measurements is very good at most locations, with a mean FD of 0.17 over all locations. This means that, on average, differences in the annual amplitude are only 17% of the value of the annual amplitude. Furthermore, there are only 7 stations where FDs > 0.5, indicating that the good agreement is uniform across tide gauge stations.

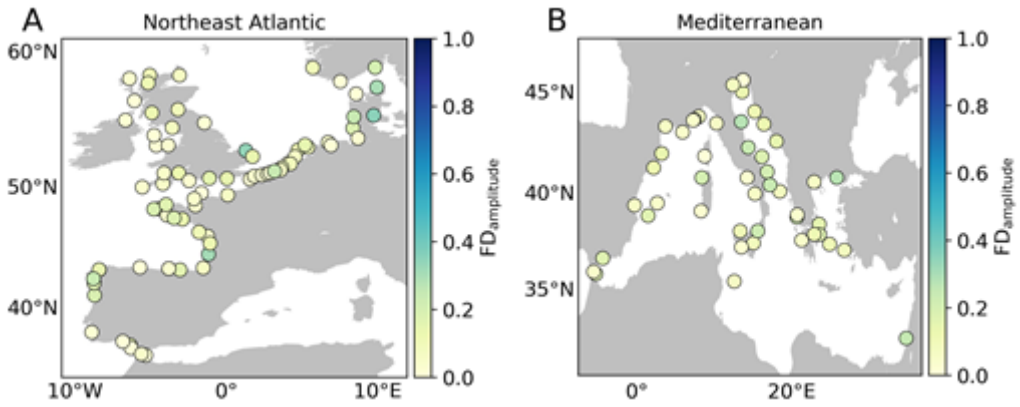

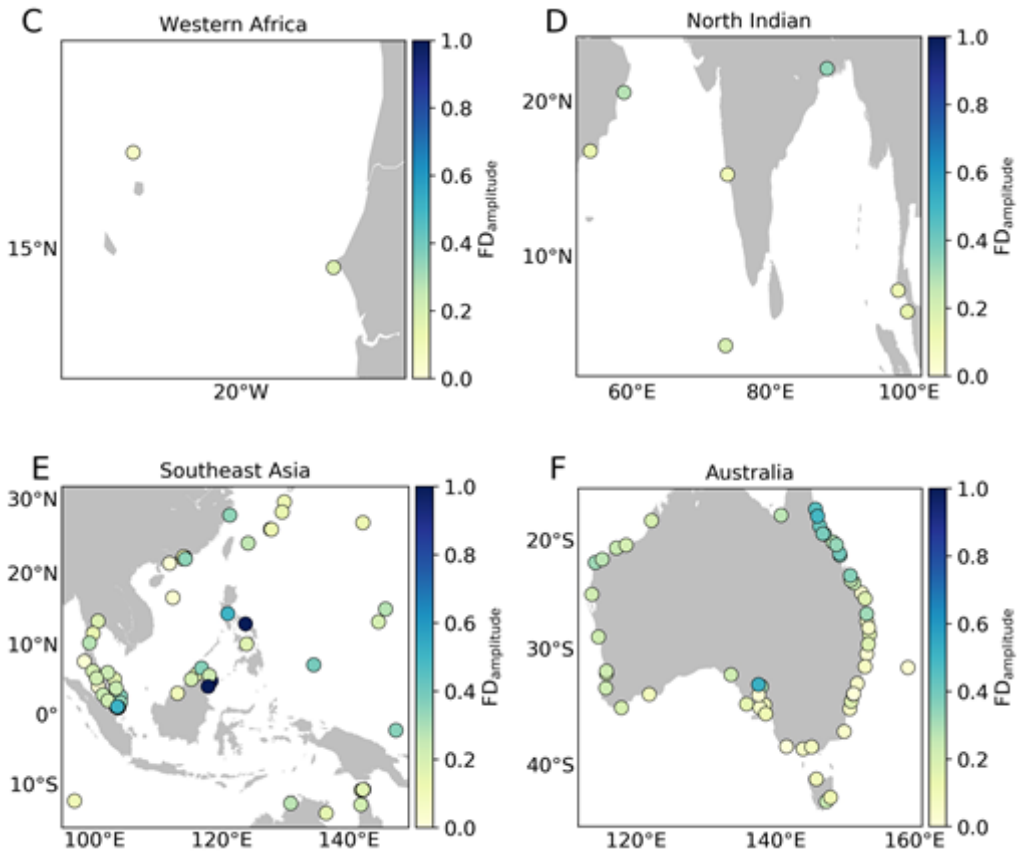

Figure 21: FDs between the amplitude of the sea-level annual cycle from tide gauge records and from satellite altimetry (the 'best' timeseries computed as described in Section 5.3.3) in (A) the Northeast Atlantic Ocean, (B) the Mediterranean Sea, (C) the Western African coast, (D) the North Indian Ocean, (E) Southeast Asian, and (F) Australia.

Trends

The assessment of trends is conducted in terms of FDs relative to the standard errors associated with the trend estimates, as described in Section 5.3.3. The interpretation of the FDs is such that FDs>1 indicate that the trends from altimetry and the tide gauges are likely to be different from a statistical point of view, otherwise we would say that they are statistically consistent. We find that FDs can differ greatly across stations with values ranging from almost 0 to more than 6 (Figure 22), indicating that signals with short lengths scales can have an important contribution to the sea-level trends at many locations over short periods such as the one considered here (<17 years). In particular, local VLMs that are not captured by relatively distant GPS stations are likely to play an important role in explaining the differences in trend between the tide gauge and altimetry estimates. In spite of the large spread in the FDs, the median FD over all stations is 0.67 and 0.58 when we include only stations where a GPS adjustment is made, which implies that there is a very good match between the altimetry and tide gauge trends at half of the stations. FDs < 1 are found at 162 stations out of 248, which means that the trends are statistically consistent at a majority of stations. We note that grouping the altimetry

data according to distances to the coast does not in general improve the agreement with the tide gauges compared to using all the altimetry data that falls within the estimated length scales.

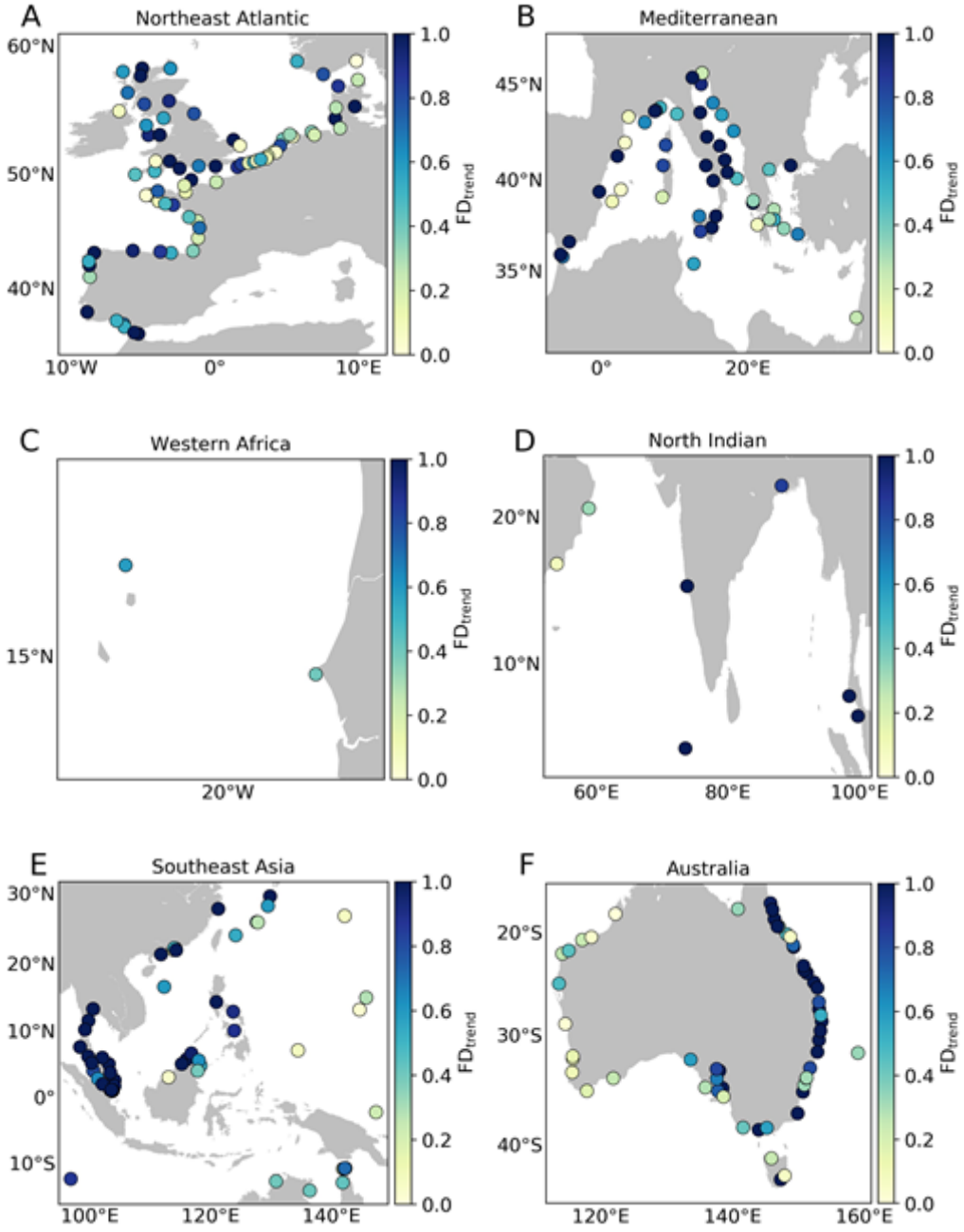

Figure 22: FDs between the sea-level trends from tide gauge records and from satellite altimetry (the 'best' timeseries computed as described in Section 5.3.3) over the period from January 2002 to May 2018 in (A) the Northeast Atlantic Ocean, (B) the Mediterranean Sea, (C) the Western African coast, (D) the North Indian Ocean, (E) Southeast Asian, and (F) Australia. Note that the colorbar has been saturated for the

sake of clarity (i.e., the range of FDs is not limited to the range from 0 to 1).

Diagnostics as a function of distance to the coast for selected stations.

In this section we show a more detailed validation, including correlations and trends as a function of distance to the coast, at six selected tide gauge stations (one in each of the six regions) (Figure 23 - Figure 28). The top-right panel in each figure displays a comparison of the 'best' monthly altimetry timeseries (computed using all the altimetry data that falls within one length scale around the tide gauge, as described in Section 5.3.3) with the sea level from the tide gauge records. There is, in general, a very good agreement between the tide gauge and altimetric timeseries and most discrepancies between the two occur at sub-annual timescales largely due to the issue of sampling uncertainty affecting the altimetry timeseries (note that the altimetry timeseries tend to show larger sub-annual variability). We note that, in most cases (77% of all tide gauges), the 'best' altimetry timeseries shows a higher correlation with the tide gauge record than any of the altimetry timeseries based on distance to the coast (see correlations in bottom-right panel). A large part of the reason for this is that when merging all the altimetry data to construct our 'best' altimetry timeseries we are able to include more values to compute the monthly means than when dividing the data according to distances to coast, which leads to a timeseries that is less affected by sampling uncertainty due to sub-monthly sea-level variability. Finally, we note that the correlation with tide gauge observations often decreases significantly at the closest points to the coast and this always should be taken as an indication that both the variability and the trends might be unreliable at such locations.

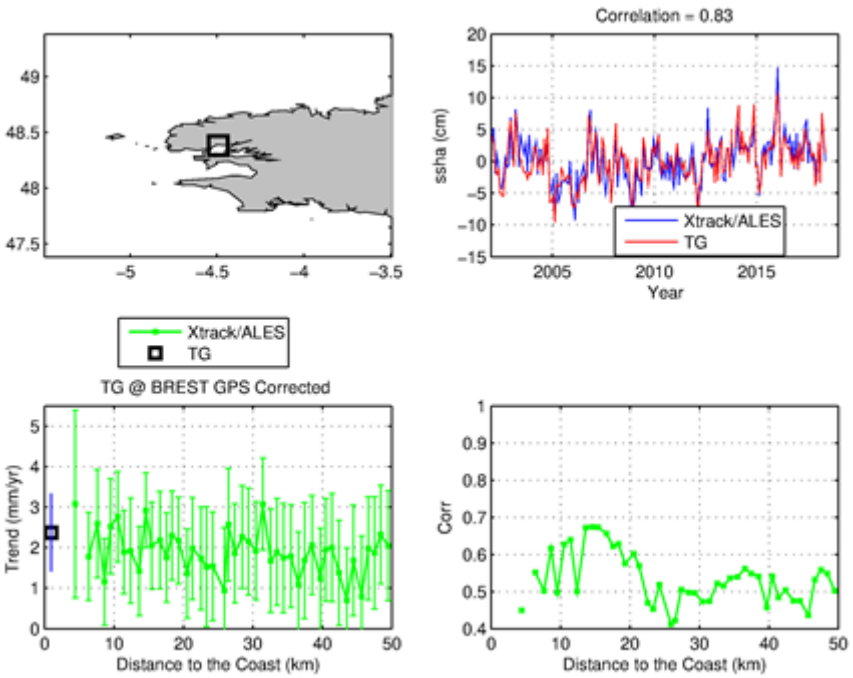

Figure 23: Validation at the Brest tide gauge. Map showing location of the tide gauge (top left), 'best' deseasoned monthly altimetry timeseries (see Section 5.3.3) compared with the monthly tide gauge record (top right), trend as a function of distance to the coast (bottom left), and correlation as a function of distance to the coast (bottom right).

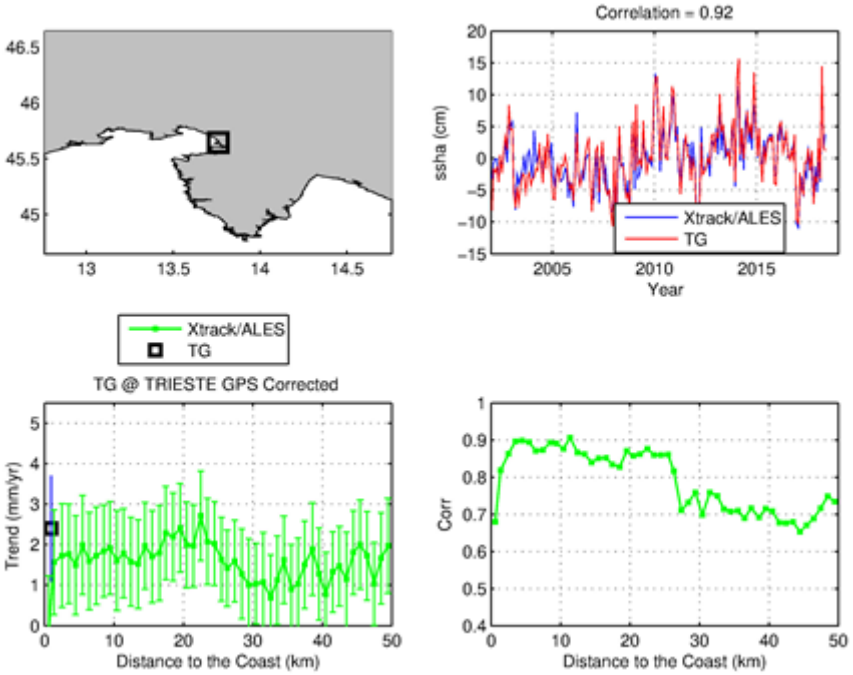

Figure 24: Same as Figure 23 but for the Trieste tide gauge.

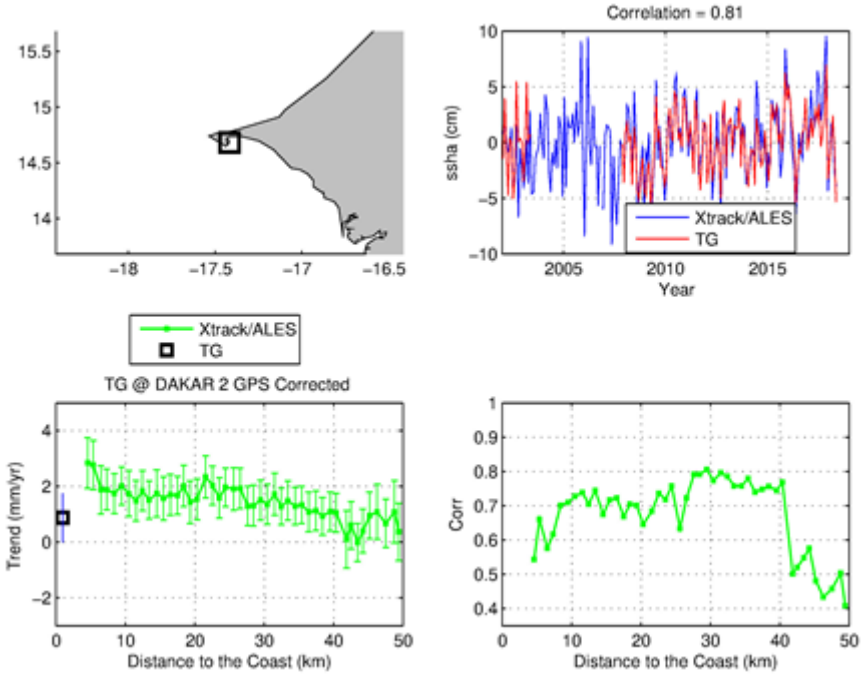

Figure 25. Same as Figure 23 but for the Dakar tide gauge.

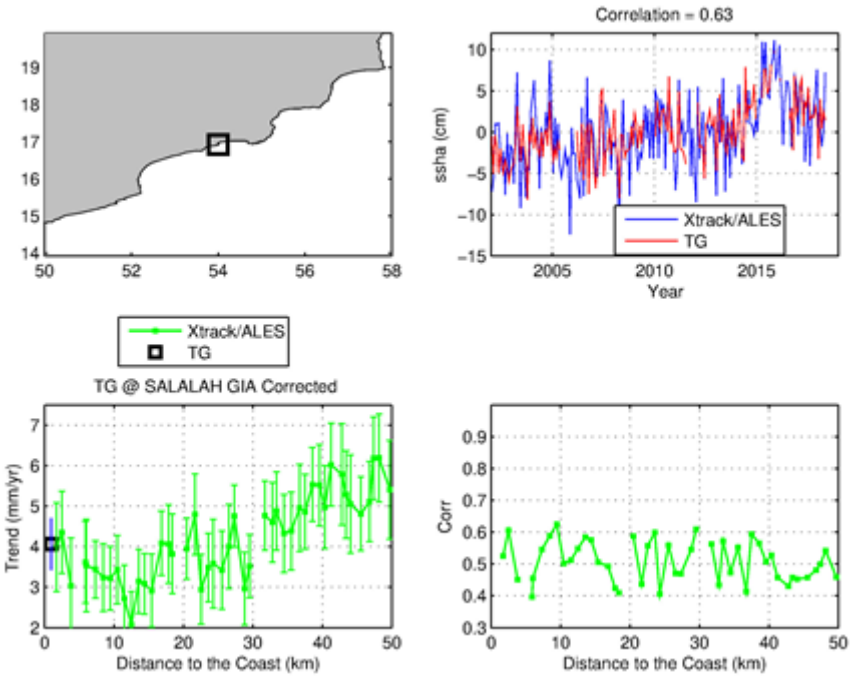

Figure 26: Same as Figure 23 but for the Salalah tide gauge.

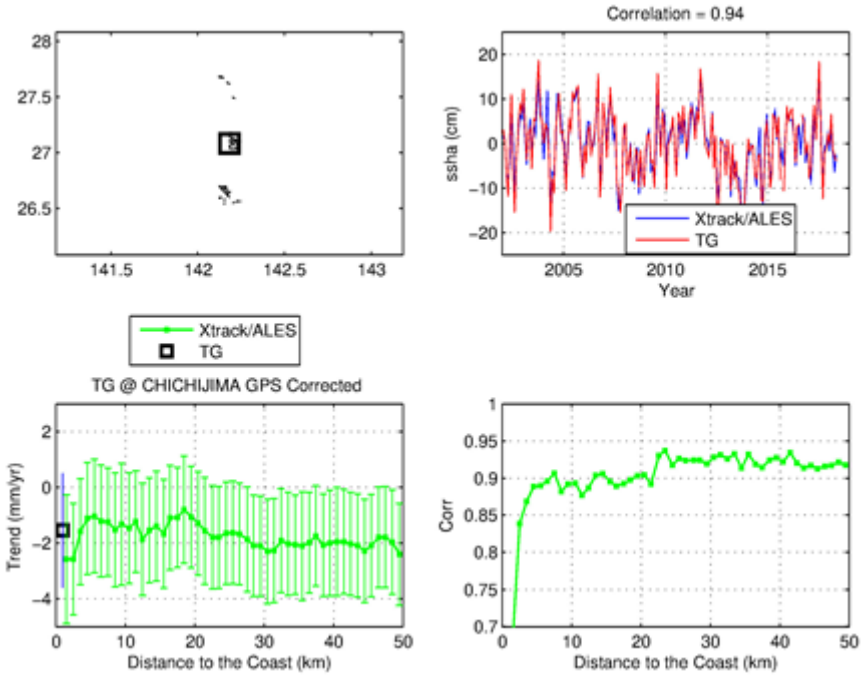

Figure 27: Same as **Figure 23** but for the Chichijima tide gauge.

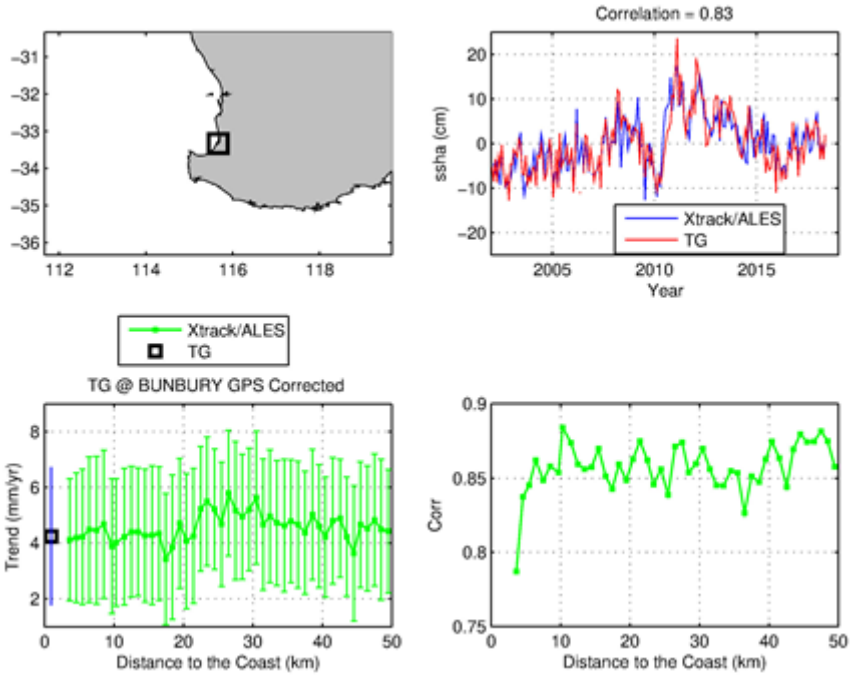

Figure 28: Same as **Figure 23** but for the Bunbury tide gauge.

5.4. Conclusions

Validating altimetry products against tide gauge observations is essential to ensuring that the products can be confidently used by the scientific community. Such validation is, however, challenging because of a number of difficulties, including sampling uncertainty due to sub-monthly variability, differences due to spatial separation and VLM at the tide gauge locations. Here, we have demonstrated that the issues of sampling uncertainty and spatial separation can be alleviated by selecting altimetry data based on the characteristic length scales of the sea-level signals around the tide gauges, allowing a more proper assessment of the altimetry data. We have found that the new SL_cci+ coastal sea-level product provides a very good agreement with tide gauge observations in terms of correlations (average of 0.77) and the sea-level annual cycle (mean FD of 0.17 for the amplitude). The agreement in terms of trends is less good, we presume largely because of the issue of VLM at tide gauge locations, but even in this case we find a median FD of 0.58 at locations where GPS data are available, which is still a good result. Our analysis as a function of distance to the coast indicates that, on average, the altimeter performance is good up to about 4 km to the coast but it tends to decline rapidly at locations closer than such distance. A final point to make is that, often, considering all the data that fall within the characteristic length scales of variability leads to a better agreement with the tide gauge data than selecting only points close to the coast, though ideally the determination of whether to use the altimetry data in one or the other way should be made on a site-by-site basis

6. Annex 2: Characterisation of uncertainties at regional scales

The goal of this WP is to estimate uncertainties associated to regional sea level trends. We use the approach developed by Ablain et al. (2019) based on the estimation of an error budget which is then used to estimate error covariance matrices. These matrices are introduced into the ordinary least squares formulation to update the distribution of model parameters, leading to a more accurate estimation of uncertainties.

Here we regionalise the error budget and perform an uncertainty estimation at each grid step. The error budget we use is summarized below:

type	description	value
correlated	short period noise	$\lambda = 1\ yr$, σ location dependent
correlated	wet tropospheric error	$\lambda = 10\ yrs$, σ location dependent
drift	orbit	$\delta = 0.33\ mm.yr^{-1}$
drift	GIA	δ location dependent
bias	TP-a/TP-b and TP-b/J1	$\sigma = 10\ mm$
bias	J1/J2 and J2/J3	$\sigma = 6\ mm$

Errors fall into three categories: biases, correlated errors or drifts. Each corresponding to a given covariance structure which is scaled to account for local error levels.

We perform an analysis to estimate the uncertainty affecting regional sea level trends and accelerations. Results are shown on Figure 1, at the 90% confidence level.

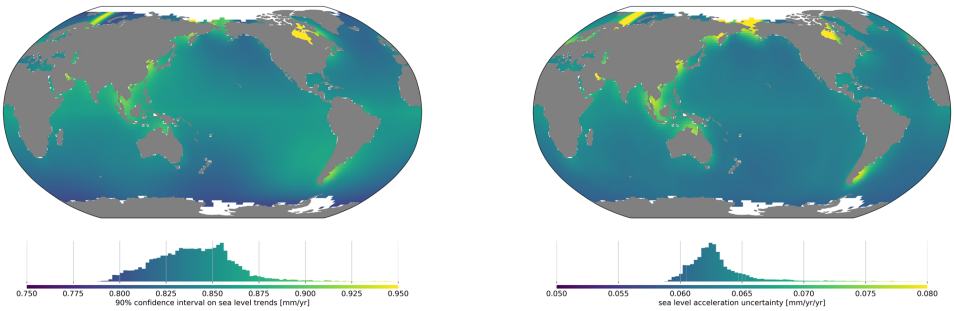

Figure 1: 90% confidence interval on regional sea level trends (left) and accelerations (right)

How much of the global ocean is experiencing significant rise or acceleration is maybe a more important information. Based on C3S sea level grids, corrected for the TOPEX-A drift, we estimate regional sea level trends and accelerations. Our results suggest that 98% of the ocean is experiencing significant rise, while 70% is experiencing a significant acceleration. The corresponding maps are shown on Figure 2. However, one should note that we consider only errors related to the altimetric system (orbit stability, measurement noises, …). As a result, significant accelerations mainly result from low frequency natural ocean variability, which is not considered in this study.

These results are presented in full details in Prandi et al., 2021.

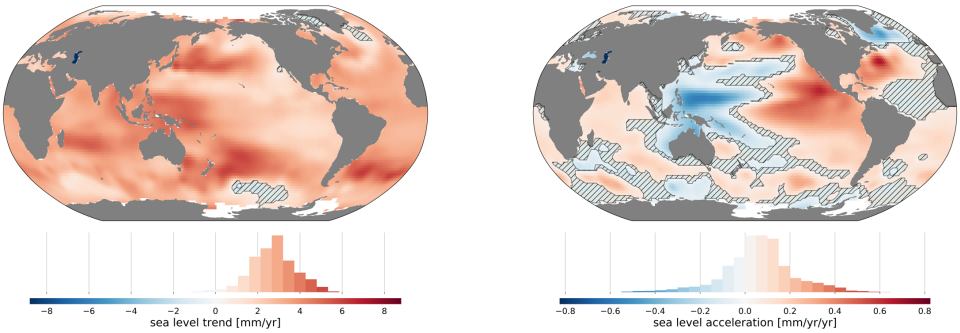

Figure 2: Maps of sea level trends (left) and accelerations (right), non-significant areas are hatched

7. References

Ablain M, Meyssignac B, Zawadzki L, Jugier R, Ribes A, Cazenave A, Picot N. 2019. Uncertainty in satellite estimate of global mean sea level changes, trend and acceleration, Earth Syst Sci Data. 11:1189–1202. DOI:10.5194/essd-11-1189-2019.

Chib S. (1993) Bayes regression with autoregressive errors. A Gibbs sampling approach J. Econometrics, 58, pp. 275-294.

Climate Change Initiative Coastal Sea Level Team, Coastal sea level anomalies and associated trends from Jason satellite altimetry over 2002-2018, *Nature Scientific Data*, Sci Data 7, 357 (2020). https://doi.org/10.1038/s41597-020-00694-w

Gouzenes Y, Leger F. Cazenave A., Birol F., Almar R., Bonnefond P., Passaro M., Legeais J.F. and Benveniste J., Coastal sea level change at Senetosa (Corsica) during the Jason altimetry missions, submitted, *Ocean Sciences*, 2020.

Holgate, S. J. et al. New data systems and products at the permanent service for mean sea level. J. Coast. Res. 29, 493–504 (2013).

Peltier W.R 2004 Global Glacial Isostasy and the Surface of the Ice-Age Earth: The ICE-5G(VM2) model and GRACE. Ann. Rev. Earth. Planet. Sci. 2004. 32,111-149.

Prandi, P., Meyssignac, B., Ablain, M., Spada, G., Ribes, A. & Benveniste, J., Local sea level trends, accelerations and uncertainties over 1993–2019. Sci Data 8, 1 (2021). https://doi.org/10.1038/s41597-020-00786-7

Prichard, D., and J. Theiler (1994), Generating surrogate data for time series with several simultaneously measured variables, Phys. Rev. Lett., 73, 951–954.

Rasmussen, C. E., C. K. I. Williams, Gaussian Processes for Machine Learning (MIT Press, Cambridge, MA, 2006).

Woodworth, P.L., Melet, A., Marcos, M. et al. Forcing Factors Affecting Sea Level Changes at the Coast. Surv. Geophys. 40, 1351–1397 (2019). https://doi.org/10.1007/s10712-019-09531-1

Wöppelmann, G., and M. Marcos (2016), Vertical land motion as a key to understanding sea level change and variability, Rev. Geophys., 54, 64–92, doi:10.1002/2015RG000502.

End of the document